

Synthesis and Structure of Intermediates in Copper-Catalyzed Alkylation of Diphenylphosphine

Matthew F. Cain,[†] Russell P. Hughes,[†] David S. Glueck,^{*,†} James A. Golen,[‡] Curtis E. Moore,[‡] and Arnold L. Rheingold[‡]

[†]6128 Burke Laboratory, Department of Chemistry, Dartmouth College, Hanover, New Hampshire 03755, and

[‡]Department of Chemistry, University of California, San Diego, 9500 Gilman Drive, La Jolla, California 92093

Received April 26, 2010

Cu(I) catalysts for alkylation of diphenylphosphine were developed. Treatment of $[\text{Cu}(\text{NCMe})_4][\text{PF}_6]$ (**1**) with chelating ligands gave $[\text{CuL}(\text{NCMe})][\text{PF}_6]$ (**2**; L = MeC(CH₂PPh₂)₃ (triphos), **3**; L = 9,9-dimethyl-4,5-bis(diphenylphosphino)-xanthene (XantPhos)). These complexes catalyzed the alkylation of PPh₂ with PhCH₂Br in the presence of the base NaOSiMe₃ to yield PPh₂CH₂Ph (**4**). The precursors Cu(dtbp)(X) (dtbp = 2,9-di-*t*-butylphenanthroline, X = Cl (**5**) or OTf (**6**)), CuCl, and **1** also catalyzed this reaction, but dtbp dissociated from **5** and **6** during catalysis. Both **2** and **3** also catalyzed alkylation of PPh₂ with PhCH₂Cl/NaOSiMe₃, but XantPhos dissociation was observed when **3** was used. When CH₂Cl₂ was used as the solvent for alkylation of PhCH₂Cl with precursors **2** or **3**, or of PhCH(Me)Br with **2**, it was competitively alkylated to yield PPh₂CH₂Cl (**7**), which was formed exclusively using **2** in the absence of a benzyl halide. Cu(triphos)-catalyzed alkylation of PhCH(Me)Br gave mostly PPh₂CHMePh (**8**), along with some Ph₂P-PPh₂ (**9**), which was also formed in attempted alkylation of dibromoethane with this catalyst. The phosphine complexes $[\text{Cu}(\text{triphos})(\text{L}')][\text{PF}_6]$ (L' = PH₂Ph (**10**), PH₂CH₂Fc (Fc = C₅H₄FeC₅H₅, **11**), PPh₂ (**12**), PHEt₂ (**13**), PHCy₂ (Cy = cyclo-C₆H₁₁, **14**), PHMe(Is) (Is = 2,4,6-(*t*-Pr)₃C₆H₂, **15**), PPh₂CH₂Ph (**16**), PPh₂CH₂Cl (**17**)), and $[\text{Cu}(\text{XantPhos})(\text{L}')][\text{PF}_6]$ (L' = PPh₂ (**18**), PPh₂CH₂Ph (**19**)) were prepared by treatment of **2** and **3** with appropriate ligands. Similarly, treatment of dtbp complexes **5** or **6** with PPh₂ gave $[\text{Cu}(\text{dtbp})(\text{PPh}_2)(\text{X})]$ (X = OTf (**20a**) or Cl (**20b**)), and reaction of PPh₂CH₂Ph (**4**) with **1** formed $[\text{Cu}(\text{PPh}_2\text{CH}_2\text{Ph})_3][\text{PF}_6]$ (**21**). Complexes **2**, **3**, **11**–**14**, **16**, **17**, **19**, and **21** were structurally characterized by X-ray crystallography. Deprotonation of diphenylphosphine complex **12** in the presence of benzyl bromide gave diphenylbenzylphosphine complex **16**, while deprotonation of **12** in CD₂Cl₂ gave **17** containing a PPh₂CD₂Cl ligand. Low-temperature deprotonation of the soluble salt **12**-[B(Ar_F)₄] (Ar_F = 3,5-(CF₃)₂C₆H₃) in THF-d₈ gave the phosphido complex Cu(triphos)(PPh₂) (**22**). Thermally unstable **22** was characterized by NMR spectroscopy and, in comparison to **12**, by density functional theory (DFT) calculations, which showed it contained a polarized Cu–P bond. The ligand substitution step required for catalytic turnover was observed on treatment of **16** or **17** with PPh₂ to yield equilibrium mixtures containing **12** and the tertiary phosphines **4** or **7**; equilibrium constants for these reactions were 8(2) and 7(2), favoring complexation of the smaller secondary phosphine in both cases. These observations are consistent with a proposed mechanism for catalytic P–C bond formation involving deprotonation of the cationic diphenylphosphine complex $[\text{Cu}(\text{triphos})(\text{PPh}_2)][\text{PF}_6]$ (**12**) by NaOSiMe₃ to yield the phosphido complex Cu(triphos)(PPh₂) (**22**). Nucleophilic attack on the substrate (benzyl halide or CH₂Cl₂) then yields the tertiary phosphine complex $[\text{Cu}(\text{triphos})(\text{PPh}_2\text{CH}_2\text{X})][\text{PF}_6]$ (X = Ph (**16**) or Cl (**17**)), and ligand substitution with PPh₂ regenerates **12**.

Introduction

We recently developed Pt catalysts for asymmetric alkylation of secondary phosphines¹ and used them for synthesis of

an enantiomerically pure DiPAMP analogue,² enantioselective tandem alkylation/arylation of primary phosphines to yield 1-phosphaacenaphthenes,³ and in studies of substrate- and catalyst-controlled selectivity in alkylation of bis(secondary

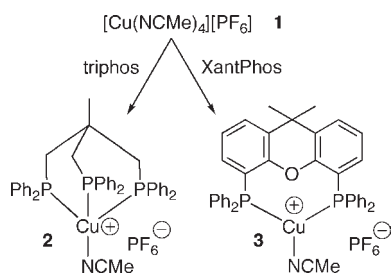
*To whom correspondence should be addressed. E-mail: glueck@dartmouth.edu.

(1) (a) Scriban, C.; Glueck, D. S. *J. Am. Chem. Soc.* **2006**, *128*, 2788–2789. (b) Scriban, C.; Glueck, D. S.; Golen, J. A.; Rheingold, A. L. *Organometallics* **2007**, *26*, 1788–1800. (Addition/Correction: Scriban, C.; Glueck, D. S.; Golen, J. A.; Rheingold, A. L. *Organometallics* **2007**, *26*, 5124). (c) Glueck, D. S. *Synlett* **2007**, 2627–2634. (d) Glueck, D. S. *Coord. Chem. Rev.* **2008**, *252*, 2171–2179.

(2) Anderson, B. J.; Glueck, D. S.; DiPasquale, A. G.; Rheingold, A. L. *Organometallics* **2008**, *27*, 4992–5001. (Addition/Correction: Anderson, B. J.; Glueck, D. S.; DiPasquale, A. G.; Rheingold, A. L. *Organometallics* **2009**, *28*, 386).

(3) Anderson, B. J.; Guino-o, M. A.; Glueck, D. S.; Golen, J. A.; DiPasquale, A. G.; Liable-Sands, L. M.; Rheingold, A. L. *Org. Lett.* **2008**, *10*, 4425–4428.

Scheme 1. Synthesis of Catalyst Precursors



phosphines).⁴ Independently, Bergman, Toste, and co-workers developed Ru catalysts for similar selective alkylations.⁵ Mechanistic studies in both systems suggested that these reactions proceeded via phosphido intermediates, and P–C bond formation occurred by nucleophilic attack of the M-PR₂ groups at alkyl halide electrophiles. Ligand substitution and proton transfer to a base then yielded the product and regenerated the catalyst. The role of the metal appeared to be two-fold: (a) it activated the phosphine substrate by making it more nucleophilic,⁶ and (b) it induced rapid pyramidal inversion at the P-stereogenic phosphido ligand,⁷ M-PR(R'), which was the origin of stereoselectivity in these reactions.⁸ Since both roles appear to be fulfilled generally across the periodic table, it is not clear that platinum group metals are required. Instead, cheaper first-row metals might make these catalysts more practical.

Here, we report development of Cu(I) catalysts, which were inspired by stoichiometric alkylation of copper(I) phosphido complexes with benzyl bromides.⁹ The weaker Cu–P bonds in these labile complexes were expected to speed up ligand substitution processes, especially in comparison to the known catalysts, which feature “inert” square planar Pt(II) and octahedral Ru(II).¹⁰ However, especially with a view to future development of asymmetric catalysts, this lability must not extend to the ancillary ligand, which must be tightly bound to avoid displacement by the phosphine substrate and products, or formation of inactive μ -phosphido dimers.¹¹ Therefore, we investigated chelate ligands such as tridentate triphos (MeC(CH₂PPh₂)₃) and bidentate XantPhos (9,9-dimethyl-4,5-bis(diphenylphosphino)xanthene) and dtbp (2,9-di-*t*-butyl-phenanthroline).

Results and Discussion

Synthesis of Catalyst Precursors. Treatment of [Cu(NCMe)₄][PF₆] (**1**) with chelating ligands gave [Cu(triphos)(NCMe)][PF₆] (**2**) and [Cu(XantPhos)(NCMe)][PF₆] (**3**) in high yields (Scheme 1).

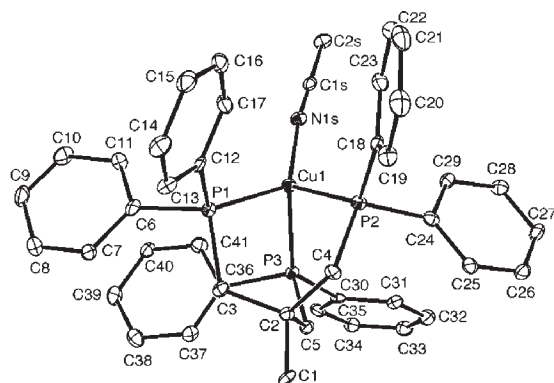


Figure 1. ORTEP diagram of the cation in one of the two independent molecules of [Cu(triphos)(NCMe)][PF₆] (**2**). Selected average bond lengths (Å) and angles (deg): Cu–N 1.939(5), Cu–P1 2.2688(17), Cu–P2 2.2540(18), Cu–P3 2.2742(17); N–Cu–P1 127.41(16), N–Cu–P2 117.91(16), N–Cu–P3 118.67(15), P1–Cu–P2 94.91(6), P2–Cu–P3 97.98(6), P1–Cu–P3 93.38(6).

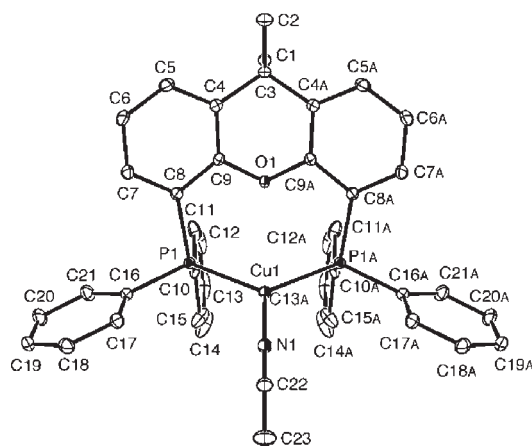


Figure 2. ORTEP diagram of the cation in [Cu(XantPhos)(NCMe)][PF₆]·2CH₂Cl₂ (**3**·2CH₂Cl₂). The anion and solvent are not shown. Selected bond lengths (Å) and angles (deg): Cu–P 2.2692(5), Cu–N 1.941(2), P–Cu–P 116.46(2), P–Cu–N 121.717(12).

The crystal structures of these complexes showed the expected pseudo-tetrahedral and trigonal planar geometries (Figures 1 and 2; see Table 1 and the Supporting Information for crystallographic details).¹²

Cu-Catalyzed Alkylation of Diphenylphosphine. Complexes **2** and **3** catalyzed the alkylation of PPh₂ with PhCH₂Br in the presence of the base¹³ NaOSiMe₃ to yield PPh₂CH₂Ph (**4**); so did the precursors Cu(dtbp)(X) (X = Cl (**5**) or OTf (**6**)),¹⁴ CuCl, and **1** (Scheme 2, Table 2, entries 1–9). Although the copper-free background reaction also occurred (Table 2, entries 10–11), the catalytic reactions (with 10 mol % loading) were faster, occurring in a few minutes. The phosphine complexes were robust, but dissociation of dtbp was observed in the reactions of **5** and **6**.

(12) For the structures of related Cu(XantPhos) complexes, see: (a) Kaltzoglou, A.; Fassler, T. F.; Aslanidis, P. *J. Coord. Chem.* **2008**, *61*, 1774–1781. (b) Huang, J.; Chan, J.; Chen, Y.; Borths, C. J.; Baucom, K. D.; Larsen, R. D.; Faul, M. M. *J. Am. Chem. Soc.* **2010**, *132*, 3674–3675.

(13) NaOSiMe₃ was used, as in related catalyses (reference 1), to reduce the rate of the background reaction by minimizing deprotonation of uncoordinated PPh₂.

(14) Gandhi, B. A.; Green, O.; Burstyn, J. N. *Inorg. Chem.* **2007**, *46*, 3816–3825.

(4) (a) Chapp, T. W.; Glueck, D. S.; Golen, J. A.; Moore, C. E.; Rheingold, A. L. *Organometallics* **2010**, *29*, 378–388. (b) Chapp, T. W.; Schoenfeld, A. J.; Glueck, D. S. *Organometallics* **2010**, *29*, 2465–2473.

(5) (a) Chan, V. S.; Stewart, I. C.; Bergman, R. G.; Toste, F. D. *J. Am. Chem. Soc.* **2006**, *128*, 2786–2787. (b) Chan, V. S.; Chiu, M.; Bergman, R. G.; Toste, F. D. *J. Am. Chem. Soc.* **2009**, *131*, 6021–6032.

(6) Glueck, D. S. *Dalton Trans.* **2008**, 5276–5286.
(7) Rogers, J. R.; Wagner, T. P. S.; Marynick, D. S. *Inorg. Chem.* **1994**, *33*, 3104–3110.

(8) Glueck, D. S. *Chem.—Eur. J.* **2008**, *14*, 7108–7117.
(9) (a) Meyer, C.; Grützmaker, H.; Pritzkow, H. *Angew. Chem., Int. Ed. Engl.* **1997**, *36*, 2471–2473. (b) Meyer, C.; Scherer, M.; Schönberg, H.; Rügger, H.; Loss, S.; Gramlich, V.; Grützmaker, H. *Dalton Trans.* **2006**, 137–148.

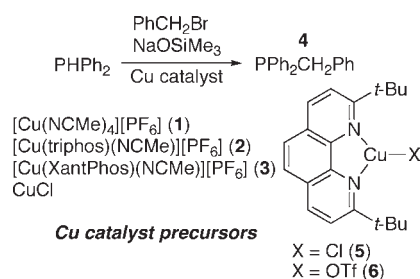
(10) Langford, C. H.; Gray, H. B. *Ligand Substitution Processes*; W. A. Benjamin: New York, 1966.

(11) Scriban, C.; Wicht, D. K.; Glueck, D. S.; Zakharov, L. N.; Golen, J. A.; Rheingold, A. L. *Organometallics* **2006**, *25*, 3370–3378.

Table 1. Crystallographic Data for the Cu Complexes **2**, **3**·2CH₂Cl₂, **11**–**14**·THF, **16**·1.5CH₂Cl₂, **17**·EtOH, and **19**·2CH₂Cl₂

compound	2	3 ·2CH ₂ Cl ₂	11	12	13	14 ·THF	16 ·1.5CH ₂ Cl ₂	17 ·EtOH	19 ·2CH ₂ Cl ₂
formula	C ₄₃ H ₄₂ CuF ₆ NP ₄	C ₄₃ H ₃₉ Cl ₄ CuF ₆ NOP ₃	C ₅₂ H ₅₂ Cu F ₆ FeP ₅	C _{54.5} H ₅₃ Cl ₃ CuF ₆ P ₅	C ₄₅ H ₅₂ CuF ₆ OP ₅	C ₅₇ H ₇₀ CuF ₆ OP ₅	C _{61.5} H ₅₉ Cl ₃ CuF ₆ P ₅	C ₅₆ H ₅₇ ClCuF ₆ OP ₅	C ₆₀ H ₅₃ Cl ₄ CuF ₆ OP ₄
formula wt	874.20	998.00	1065.18	1146.71	941.26	1103.52	1236.83	1113.86	1233.24
space group	<i>P2</i> (1)/ <i>c</i>	<i>P2</i> (1)/ <i>m</i>	<i>P2</i> (1)/ <i>n</i>	<i>P</i> $\bar{1}$	<i>P2</i> (1)/ <i>n</i>	<i>P2</i> (1)	<i>P2</i> (1)/ <i>n</i>	<i>P2</i> (1)/ <i>c</i>	<i>P</i> $\bar{1}$
<i>a</i> , Å	29.1600(11)	8.6254(12)	11.866(3)	10.3838(6)	13.0803(6)	12.1730(3)	16.0842(7)	10.627(2)	13.449(2)
<i>b</i> , Å	14.0993(6)	17.945(3)	32.018(9)	12.8816(7)	16.9559(8)	17.3557(4)	16.9120(7)	25.660(5)	13.521(2)
<i>c</i> , Å	20.7714(8)	14.093(2)	12.795(3)	21.8230(12)	21.4791(10)	12.9747(3)	21.1911(9)	19.383(4)	17.421(3)
α , deg	90	90	90	86.5950(10)	90	90	90	90	74.159(2)
β , deg	110.820(3)	96.776(4)	98.794(6)	77.5010(10)	107.3490(10)	103.3610(10)	92.301(3)	100.073(4)	70.067(2)
γ , deg	90	90	90	69.2370(10)	90	90	90	90	73.684(2)
<i>V</i> , Å ³	7982.2(5)	2166.0(5)	4804(2)	2664.3(3)	4547.1(4)	2666.98(11)	5759.7(4)	5204.0(19)	2802.5(8)
<i>Z</i>	8	2	4	2	4	2	4	4	2
<i>D</i> (calcd), g/cm ³	1.455	1.530	1.473	1.429	1.375	1.374	1.426	1.422	1.461
μ (MoK α), mm ⁻¹	2.811 ^a	0.924	0.971	0.768	0.714	2.500 ^a	3.621 ^a	0.686	0.756
temp, K	100(2)	100(2)	150(2)	100(2)	100(2)	100(2)	120(2)	100(2)	100(2)
<i>R</i> (<i>F</i>), % ^b	4.99	3.09	4.47	5.93	4.06	3.65	5.58	6.43	8.06
<i>R</i> _w (<i>F</i> ²), % ^b	11.97	8.04	9.68	14.43	10.95	9.58	14.89	13.38	21.66

^a Cu K α radiation was used. ^b Quantity minimized: $R_w(F^2) = [\sum w(F_o^2 - F_c^2)^2 / \sum w(F_o^2)^2]^{1/2}$; $R = \sum \Delta / \sum (F_o)$, $\Delta = |(F_o - F_c)|$, $w = 1/[\sigma^2(F_o^2) + (aP)^2 + bP]$, $P = [2F_c^2 + \text{Max}(F_o^2, 0)]/3$. A Bruker CCD diffractometer was used in all cases.

Scheme 2. Cu-Catalyzed Alkylation of PPh₂ with PhCH₂Br

Triphos complex **2** also catalyzed alkylation of PPh₂ with benzyl chloride in tetrahydrofuran (THF) or CH₂Cl₂ to yield **4** (Scheme 3, Table 2, entries 12–13). This reaction was slower than alkylation with PhCH₂Br, but the even slower background process was now insignificant (Table 2, entries 16–17). When XantPhos precursor **3** was used, **4** was also formed, but XantPhos dissociation was observed (Table 2, entries 14–15).

When methylene chloride was used as the solvent for reactions of benzyl chloride, it was competitively alkylated to yield mixtures of **4** and the known chloromethylphosphine PPh₂CH₂Cl (**7**; Table 2, entries 12 and 14).¹⁵ In contrast, alkylation of diphenylphosphine with benzyl bromide proceeded smoothly in CH₂Cl₂ with **2**, **3**, or other catalyst precursors (Table 2, entries 1–3, 5, and 7–9). When no benzyl halide was added, Cu(triphos)-catalyzed alkylation of methylene chloride solvent gave **7** in high yield (Scheme 3, Table 2, entry 18; no background reaction occurred (entry 19)). Although such a stoichiometric reaction was reported for a Re phosphido complex, this is the first observation of catalysis.¹⁶

Alkylation by the CH₂Cl₂ solvent to yield **7** also occurred in the Cu(triphos)-catalyzed reaction of PPh₂ with the more hindered benzyl bromide PhCH(Me)Br, which gave PPh₂CHMePh (**8**) as the major product¹⁷ along with PPh₂CH₂Cl (**7**) and the biphosphine Ph₂P-PPh₂ (**9**; Table 2, entry 21). Only **8** and **9** were formed in THF, much faster than in the background reaction (Scheme 4; Table 2, entries 20 and 22). Cu(triphos)-mediated alkylation of PhCH(Me)Cl was much slower, yielding mostly **8** along with a small amount of **9**; triphos dissociation was also observed (Table 2, entries 23–24).

Biphosphine **9** was formed cleanly in Cu-catalyzed reaction of PPh₂ with dibromoethane in THF or CH₂Cl₂ (Scheme 5; Table 2, entries 25–27). Several related reactions of phosphido anions with dibromoethane and related alkyl or aryl halides are known; they have been proposed to occur via nucleophilic attack on halogen instead of the “normal” S_N2 attack at carbon.¹⁸

We have not investigated the ligand effects on the reactions in Table 2 in detail. However, the success of the presumably tridentate triphos ligand, and the dissociation observed for bidentate XantPhos and dtbp suggested that strong chelation by a polydentate ligand was important to stabilize catalytic intermediates.

Mechanism of Cu-Catalyzed Alkylation of Diphenylphosphine. We hypothesized that these reactions proceeded by the catalytic cycle shown in Scheme 6, in which benzyl bromide is shown as a sample electrophile.

(15) (a) Braussaud, N.; Ruther, T.; Cavell, K. J.; Skelton, B. W.; White, A. H. *Synthesis* **2001**, 626–632. (b) Burck, S.; van Assema, S. G. A.; Lastdrager, B.; Slootweg, J. C.; Ehlers, A. W.; Otero, J. M.; Dacunha-Marinho, B.; Llamas-Saiz, A. L.; Mar, O.; van Raaij, M. J.; Lammertsma, K. *Chem.—Eur. J.* **2009**, *15*, 8134–8145.

(16) (a) Buhro, W. E.; Georgiou, S.; Hutchinson, J. P.; Gladysz, J. A. *J. Am. Chem. Soc.* **1985**, *107*, 3346–3348. (b) Buhro, W. E.; Zwick, B. D.; Georgiou, S.; Hutchinson, J. P.; Gladysz, J. A. *J. Am. Chem. Soc.* **1988**, *110*, 2427–2439.

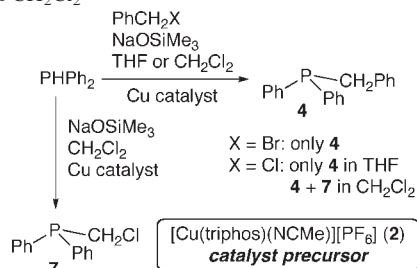
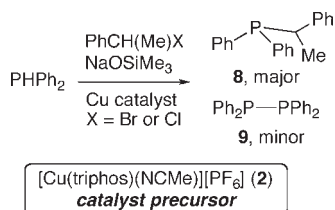
(17) (a) Heydenreich, F.; Mollbach, A.; Wilke, G.; Dreeskamp, H.; Hoffmann, E. G.; Schroth, G.; Seevogel, K.; Stempfle, W. *Isr. J. Chem.* **1972**, *10*, 293–319. (b) Millauer, H.; Brungs, P. U.S. 5808163, 1998. (c) Berens, U. EP 1582527A1, 2005.

(18) (a) Seyferth, D.; Wood, T. G.; Henderson, R. S. *J. Organomet. Chem.* **1987**, *336*, 163–182. (b) Gillespie, D. G.; Walker, B. J. *Tetrahedron Lett.* **1975**, *16*, 4709–4710. (c) Gillespie, D. G.; Walker, B. J.; Stevens, D.; McAuliffe, C. A. *J. Chem. Soc., Perkin Trans. 1* **1983**, 1697–1703. (d) Gillespie, D. G.; Walker, B. J. *J. Chem. Soc., Perkin Trans. 1* **1983**, 1689–1695. (e) Hewertson, W.; Taylor, I. C.; Trippett, S. *J. Chem. Soc. C* **1970**, 1835–1839. (f) Hewertson, W.; Taylor, I. C. *J. Chem. Soc. D* **1970**, 119–120. (g) Issleib, K.; Müller, D.-W. *Chem. Ber.* **1959**, *92*, 3175–3182. (h) Issleib, K.; Döll, G. *Chem. Ber.* **1961**, *94*, 2664–2669. (i) Issleib, K.; Döll, G. *Chem. Ber.* **1963**, *96*, 1544–1550.

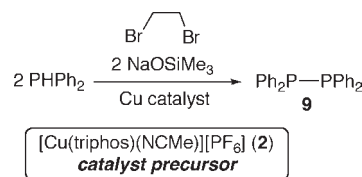
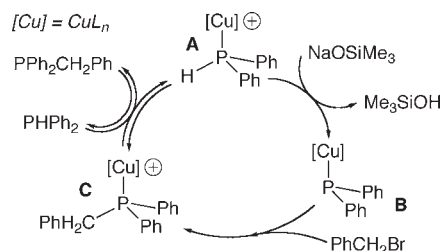
Table 2. Cu-Catalyzed Alkylation of Diphenylphosphine^a

entry	catalyst precursor	substrate	product	solvent	time	yield (%)
1	[Cu(NCMe) ₄][PF ₆] (1)	PhCH ₂ Br	PPh ₂ CH ₂ Ph (4)	CH ₂ Cl ₂	15 min	73
2	[Cu(triphos)(NCMe)][PF ₆] (2)	PhCH ₂ Br	PPh ₂ CH ₂ Ph (4)	CH ₂ Cl ₂	< 10 min	82
3	[Cu(triphos)(NCMe)][PF ₆] (2) ^b	PhCH ₂ Br	PPh ₂ CH ₂ Ph (4)	CH ₂ Cl ₂	2 h	87
4	[Cu(triphos)(NCMe)][PF ₆] (2)	PhCH ₂ Br	PPh ₂ CH ₂ Ph (4)	THF	< 15 min	89
5	[Cu(XantPhos)(NCMe)][PF ₆] (3)	PhCH ₂ Br	PPh ₂ CH ₂ Ph (4)	CD ₂ Cl ₂	< 15 min	81
6	[Cu(XantPhos)(NCMe)][PF ₆] (3)	PhCH ₂ Br	PPh ₂ CH ₂ Ph (4)	THF	< 15 min	98
7	Cu(dtbp)(Cl) (5) ^c	PhCH ₂ Br	PPh ₂ CH ₂ Ph (4)	CD ₂ Cl ₂	< 15 min	<i>d</i>
8	Cu(dtbp)(OTf) (6) ^e	PhCH ₂ Br	PPh ₂ CH ₂ Ph (4)	CD ₂ Cl ₂	< 15 min	<i>d</i>
9	CuCl	PhCH ₂ Br	PPh ₂ CH ₂ Ph (4) Ph ₂ P-PPh ₂ (9)	CH ₂ Cl ₂	15 min	84 ^f
10	none	PhCH ₂ Br	PPh ₂ CH ₂ Ph (4) [PPh ₂ (CH ₂ Ph) ₂][Br]	CD ₂ Cl ₂	15 min	<i>g</i>
11	none	PhCH ₂ Br	PPh ₂ CH ₂ Ph (4) [PPh ₂ (CH ₂ Ph) ₂][Br]	THF	15 min	<i>h</i>
12	[Cu(triphos)(NCMe)][PF ₆] (2)	PhCH ₂ Cl	PPh ₂ CH ₂ Ph (4) PPh ₂ CH ₂ Cl (7)	CH ₂ Cl ₂	1 h	75 ⁱ
13	[Cu(triphos)(NCMe)][PF ₆] (2)	PhCH ₂ Cl	PPh ₂ CH ₂ Ph (4)	THF	15 min	93
14	[Cu(XantPhos)(NCMe)][PF ₆] (3)	PhCH ₂ Cl	PPh ₂ CH ₂ Ph (4) PPh ₂ CH ₂ Cl (7)	CH ₂ Cl ₂	15 min	75 ^{j,k}
15	[Cu(XantPhos)(NCMe)][PF ₆] (3)	PhCH ₂ Cl	PPh ₂ CH ₂ Ph (4)	THF	27 h	100 ^k
16	none	PhCH ₂ Cl	PPh ₂ CH ₂ Ph (4)	CD ₂ Cl ₂	72 h	<i>l</i>
17	none	PhCH ₂ Cl	PPh ₂ CH ₂ Ph (4)	THF	3 h	<i>m</i>
18	[Cu(triphos)(NCMe)][PF ₆] (2)	CH ₂ Cl ₂	PPh ₂ CH ₂ Cl (7)	CH ₂ Cl ₂	25 min	86
19	none	CH ₂ Cl ₂	PPh ₂ CH ₂ Cl (7)	CH ₂ Cl ₂	48 h	0 ⁿ
20	[Cu(triphos)(NCMe)][PF ₆] (2)	PhCH(Me)Br	PPh ₂ CH(Me)Ph (8) Ph ₂ P-PPh ₂ (9)	THF	15 min	100 ^o
21	[Cu(triphos)(NCMe)][PF ₆] (2)	PhCH(Me)Br	PPh ₂ CH(Me)Ph (8) PPh ₂ CH ₂ Cl (7) Ph ₂ P-PPh ₂ (9)	CH ₂ Cl ₂	20 min	<i>p</i>
22	none	PhCH(Me)Br	PPh ₂ CH(Me)Ph (8) Ph ₂ P-PPh ₂ (9)	THF	15 min	<i>q</i>
23	[Cu(triphos)(NCMe)][PF ₆] (2)	PhCH(Me)Cl	PPh ₂ CH(Me)Ph (8)	THF	72 h	74 ^r
24	none	PhCH(Me)Cl	PPh ₂ CH(Me)Ph (8)	THF	75 h	<i>s</i>
25	[Cu(triphos)(NCMe)][PF ₆] (2)	Br(CH ₂) ₂ Br	Ph ₂ P-PPh ₂ (9)	THF	15 min	77 ^t
26	[Cu(triphos)(NCMe)][PF ₆] (2)	Br(CH ₂) ₂ Br	Ph ₂ P-PPh ₂ (9)	CH ₂ Cl ₂	15 min	71 ^u
27	none	Br(CH ₂) ₂ Br	Ph ₂ P-PPh ₂ (9)	THF	15 min	<i>v</i>

^a Standard conditions for catalytic alkylation: 50 mg of PPh₂ (0.27 mmol), 1 equiv of electrophile, 10 mol % Cu catalyst precursor, 2 mL of solvent, 1 equiv of NaOSiMe₃. Reactions were monitored by ³¹P NMR spectroscopy, then worked up as described in the Experimental Section and Supporting Information. Isolated yields are reported. ^b 1 mol % catalyst precursor. ^c 0.51 mmol of PPh₂. ^d Phosphine **4** was the only product observed by ³¹P NMR, but the ¹H NMR spectrum showed free dtbp. ^e 0.47 mmol of PPh₂. ^f Mostly **4**, with a trace of **9**. ^g 22% conversion; 2:1 ratio of **4** to the salt [PPh₂(CH₂Ph)₂][Br]. ^h 61% conversion to a mixture of **4** and the salt [PPh₂(CH₂Ph)₂][Br] (25:1). ⁱ 93:7 mixture of **4** and **7** (88:12 before workup). ^j 97:3 mixture of **4** and **7**. ^k XantPhos dissociation was observed. ^l < 5% conversion. ^m 5% conversion; 14% conversion after 16.5 h. ⁿ No reaction occurred. ^o 97:3 ratio of **8** to **9** before and after workup. ^p The initial ratio of **8**:**7**:**9** was 68:28:4. ^q After 15 min, about 16% conversion to a 2.5:1 mixture of **8** and **9**. ^r triphos dissociation was observed. Phosphine **8** was obtained in 94% purity, containing **9**, triphos, and another unidentified byproduct ($\delta = -21.4$) ^s 3% conversion. ^t Contained traces of Ph₂P-PPh₂(O), PPh₂, and another unidentified byproduct. ^u Contained a trace of Ph₂P-PPh₂(O). ^v ca. 1% conversion; even after 48 h, only 2% conversion of PPh₂.

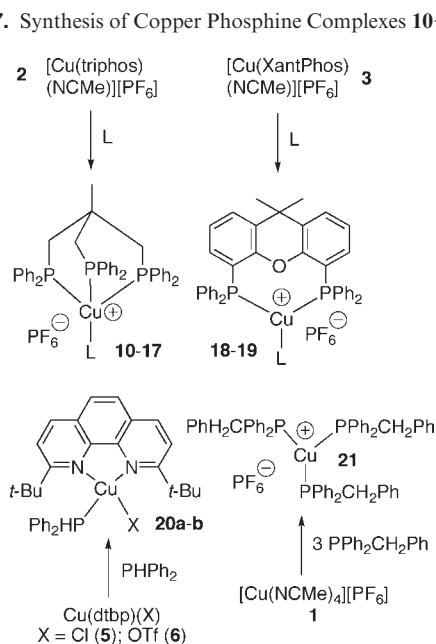
Scheme 3. Cu(triphos)-Catalyzed Alkylation of PPh₂ with Benzyl Halides and CH₂Cl₂**Scheme 4.** Cu(triphos)-Catalyzed Reactions of PPh₂ with Secondary Benzyl Halides

Reaction of a catalyst precursor, like **2** or **3**, with the phosphine substrate was expected to yield a cationic secondary phosphine complex **A**, which on deprotonation by NaOSiMe₃ would yield a nucleophilic phosphido intermediate (**B**). Attack on the electrophilic substrate,

Scheme 5. Cu(triphos)-Catalyzed Reaction of PPh₂ with Dibromoethane**Scheme 6.** Hypothetical Mechanism of Cu-Catalyzed Alkylation of PPh₂ with Benzyl Bromide

such as a benzyl halide, would yield a cationic tertiary phosphine complex (**C**). Finally, ligand substitution on **C** would regenerate **A**. To investigate these steps, we prepared examples of the proposed intermediates.

Intermediates A and C (Cationic Phosphine Complexes). The phosphine complexes [Cu(triphos)(L')][PF₆] (L' = Ph₂Ph (**10**), Ph₂CH₂Fc (Fc = C₅H₄FeC₅H₅, **11**), PPh₂

Scheme 7. Synthesis of Copper Phosphine Complexes 10–21^a

^a Ligands L: PH_2Ph (**10**), $\text{PH}_2\text{CH}_2\text{Fc}$ (**11**), PPh_2 (**12** and **18**), PHEt_2 (**13**), PHCy_2 (**14**), $\text{PHMe}(\text{Is})$ (**15**), $\text{PPh}_2\text{CH}_2\text{Ph}$ (**16** and **19**), $\text{PPh}_2\text{CH}_2\text{Cl}$ (**17**). For **20a**, $\text{X} = \text{OTf}$; for **20b**, $\text{X} = \text{Cl}$.

(**12**), PHEt_2 (**13**), PHCy_2 ($\text{Cy} = \text{cyclo-C}_6\text{H}_{11}$, **14**), $\text{PHMe}(\text{Is})$ ($\text{Is} = 2,4,6\text{-}(i\text{-Pr})_3\text{C}_6\text{H}_2$, **15**), $\text{PPh}_2\text{CH}_2\text{Ph}$ (**16**), $\text{PPh}_2\text{CH}_2\text{Cl}$ (**17**), and $[\text{Cu}(\text{XantPhos})(\text{L})][\text{PF}_6]$ ($\text{L} = \text{PPh}_2$ (**18**), $\text{PPh}_2\text{CH}_2\text{Ph}$ (**19**)) were prepared by treatment of **2** and **3** with appropriate ligands. Similarly, reaction of dtbp complexes **5** or **6** with PPh_2 gave $[\text{Cu}(\text{dtbp})(\text{PPh}_2)\text{X}]$ ($\text{X} = \text{OTf}$ (**20a**), Cl (**20b**)), and reaction of $\text{PPh}_2\text{CH}_2\text{Ph}$ (**4**) with **1** formed $[\text{Cu}(\text{PPh}_2\text{CH}_2\text{Ph})_3][\text{PF}_6]$ (**21**) (Scheme 7).

Spectroscopic characterization of these complexes was, in most cases, straightforward. The PH groups in the primary and secondary phosphine complexes were useful spectroscopic probes, with J_{PH} coupling constants of about 300–400 Hz and IR PH stretching vibrations in the range 2300–2400 cm^{-1} .¹⁹ Phosphine binding to copper resulted in large ³¹P NMR coordination chemical shifts, with broad ³¹P NMR signals due to the quadrupolar ⁶⁵Cu and ⁶³Cu nuclei.²⁰

However, the structures of the diphenylphosphine complexes of XantPhos (**18**) and dtbp (**20**) were less easy to identify. Elemental analysis and mass spectrometry were consistent with the formula of **18**. The three-coordinate structure of its $\text{PPh}_2\text{CH}_2\text{Ph}$ analogue **19** was established by its ³¹P NMR spectrum, which included a doublet and a triplet ($J_{\text{PP}} = 98$ Hz), and by X-ray crystallography (see below). However, room-temperature NMR spectra of **18** contained very broad signals, and cooling the sample did not simplify them. This behavior might result from rapid exchange with a small amount of PPh_2 . For dtbp complex **20**, the bulky ligand was expected to promote formation of three-coordinate cations $[\text{Cu}(\text{dtbp})(\text{PPh}_2)\text{X}]$, as observed in the structures of the precursors $\text{Cu}(\text{dtbp})(\text{X})$ ($\text{X} = \text{Cl}$ (**5**), OTf (**6**)).¹⁴

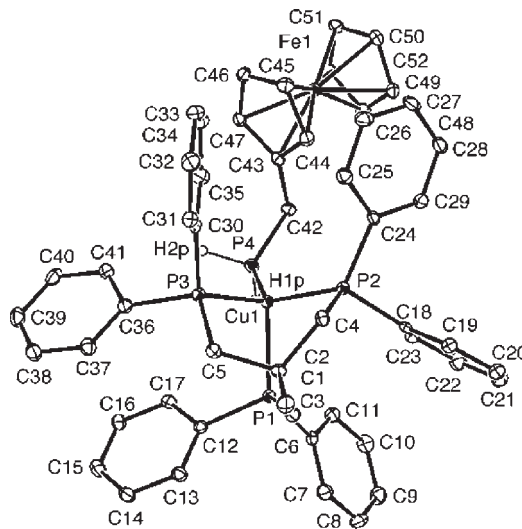


Figure 3. ORTEP diagram of the cation in $[\text{Cu}(\text{triphos})(\text{PH}_2\text{CH}_2\text{Fc})][\text{PF}_6]$ (**11**). Only the PH hydrogen atoms, which were located and refined, are shown.

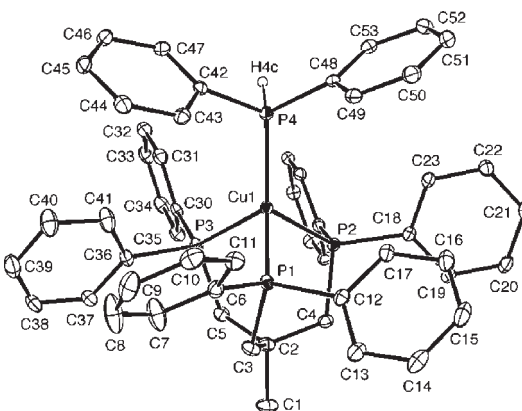


Figure 4. ORTEP diagram of the cation in $[\text{Cu}(\text{triphos})(\text{PPh}_2)][\text{PF}_6]$ (**12**). Only the PH hydrogen atom, which was located and refined, is shown.

However, the ³¹P and ¹H NMR spectra of **20a** ($\text{X} = \text{OTf}$) and **20b** ($\text{X} = \text{Cl}$) in CD_2Cl_2 were markedly different, suggesting that the anion X was bound to copper in one or both complexes. The conductivities of $\sim 1 \times 10^{-3}$ M solutions of **20a**, **20b**, and $[\text{Cu}(\text{dtbp})(\text{NCMe})_2][\text{PF}_6]$ ¹⁴ in nitromethane were 139, 54, and 149 $\Omega^{-1} \text{cm}^2 \text{mol}^{-1}$, respectively, consistent with an ionic three-coordinate structure for triflate complex **20a** and with the presence of both three- and four-coordinate forms of chloride **20b** in this polar solvent.²¹ For simplicity, Scheme 7 shows **20** as four-coordinate, but this likely depends on the anion and the solvent.

Complexes **11–14**, **16–17**, **19**, and **21** were structurally characterized by X-ray crystallography (Figures 3–9; see Tables 1 and 3 and the Supporting Information for more details and the structure of **21**).

Although the steric and electronic properties of the monodentate ligands in the complexes $[\text{Cu}(\text{triphos})(\text{L})][\text{PF}_6]$

(19) Kourkine, I. V.; Maslennikov, S. V.; Ditchfield, R.; Glueck, D. S.; Yap, G. P. A.; Liable-Sands, L. M.; Rheingold, A. L. *Inorg. Chem.* **1996**, *35*, 6708–6716.

(20) Black, J. R.; Levason, W.; Spicer, M. D.; Webster, M. J. *Chem. Soc., Dalton Trans.* **1993**, 3129–3136.

(21) (a) Geary, W. J. *Coord. Chem. Rev.* **1971**, *7*, 81–122. (b) Tye, J. W.; Weng, Z.; Giri, R.; Hartwig, J. F. *Angew. Chem., Int. Ed.* **2010**, *49*, 2185–2189. (c) Tye, J. W.; Weng, Z.; Johns, A. M.; Incarvito, C. D.; Hartwig, J. F. *J. Am. Chem. Soc.* **2008**, *130*, 9971–9983.

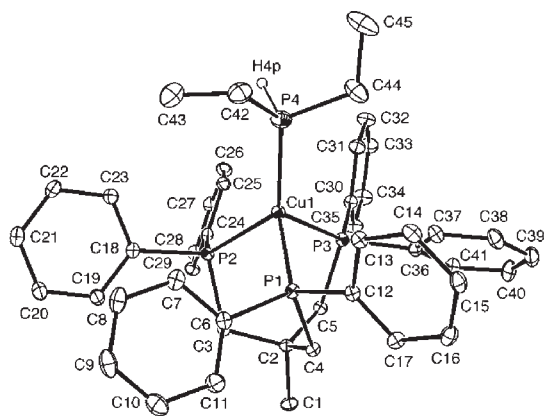


Figure 5. ORTEP diagram of the cation in $[\text{Cu}(\text{triphos})(\text{PHEt}_2)][\text{PF}_6]$ (**13**). Only the PH hydrogen atom, which was located and refined, is shown.

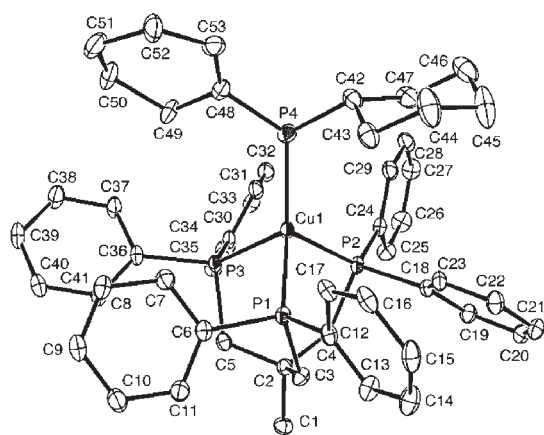


Figure 6. ORTEP diagram of the cation in $[\text{Cu}(\text{triphos})(\text{PHCy}_2)]\text{PF}_6 \cdot \text{THF}$ (**14**·THF). The solvent and disorder in a cyclohexyl group are not shown.

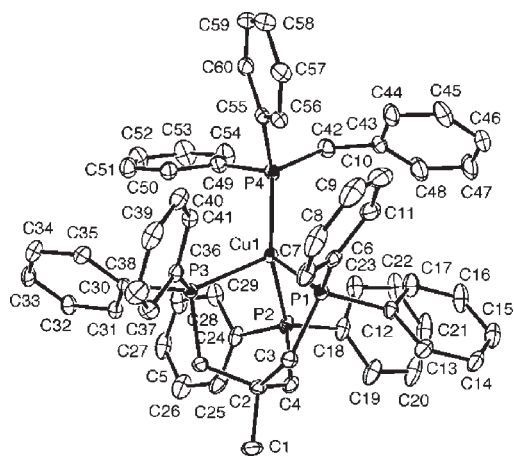


Figure 7. ORTEP diagram of the cation in $[\text{Cu}(\text{triphos})(\text{PPh}_2\text{CH}_2\text{Ph})]\text{PF}_6 \cdot 1.5\text{CH}_2\text{Cl}_2$ (**16**· $1.5\text{CH}_2\text{Cl}_2$). The solvent is not shown.

varied, the data in Table 3 showed that the crystal structures were similar, with the expected pseudo-tetrahedral geometry at copper. On replacing the P–H substituent in **12** with a P–CH₂Ph or P–CH₂Cl group in **16** or **17**, all the Cu–P bond lengths increased slightly, consistent with increased steric hindrance in the tertiary

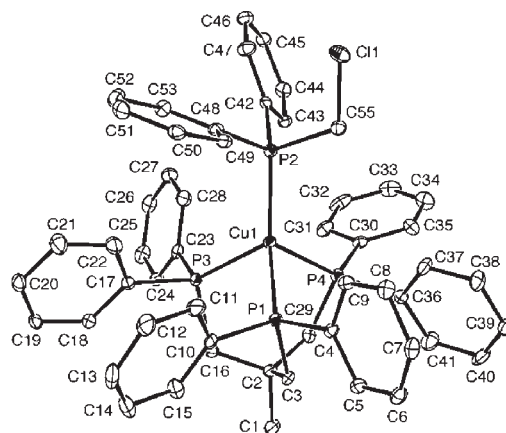


Figure 8. ORTEP diagram of the cation in $[\text{Cu}(\text{triphos})(\text{PPh}_2\text{CH}_2\text{Cl})]\text{PF}_6 \cdot \text{EtOH}$ (**17**·EtOH). The solvent is not shown.

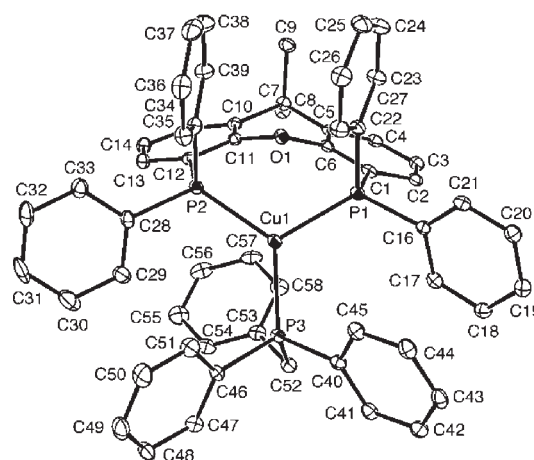


Figure 9. ORTEP diagram of the cation in $[\text{Cu}(\text{XantPhos})(\text{PPh}_2\text{CH}_2\text{Ph})]\text{PF}_6 \cdot 2\text{CH}_2\text{Cl}_2$ (**19**· $2\text{CH}_2\text{Cl}_2$). The solvent is not shown.

phosphine complexes, as also seen in the recently reported structure of $[\text{Cu}(\text{triphos})(\text{PPh}_3)]\text{BF}_4$.²²

The structure of **12** was also investigated by density functional theory (DFT) calculations. As shown in Table 3, the crystallographic structure of **12** was in excellent agreement with the computed one. Although the DFT results overestimated the Cu–P bond lengths by about 0.1 Å, they reproduced the crystallographically established trend that the Cu–P(PHPh₂) bond was slightly shorter than the Cu–P(triphos) bonds, and they also matched the angles at copper well. An overlay of the crystallographic and DFT structures of the cation of **12** is included in the Supporting Information.

Intermediate B (Terminal Cu-Phosphido Complexes). Formation by Deprotonation of Cationic Phosphine Complexes and Reaction with Electrophiles. No isolable neutral terminal Cu-phosphido complexes have been reported,^{23–25} so we expected proposed intermediates **B** to be

(22) Yin, Q.; Gan, X. *Acta Crystallogr.* **2010**, E66, m369.

(23) For anionic terminal phosphido copper complexes, see: (a) Cowley, A. H.; Giolando, D. M.; Jones, R. A.; Nunn, C. M.; Power, J. M. *J. Chem. Soc., Chem. Commun.* **1988**, 208–209. (b) Martin, S. F.; Fishpaugh, J. R.; Power, J. M.; Giolando, D. M.; Jones, R. A.; Nunn, C. M.; Cowley, A. H. *J. Am. Chem. Soc.* **1988**, 110, 7226–7228.

Table 3. Selected Bond Lengths (Å) and Angles (deg) in the Cationic Complexes [Cu(triphos(L))][PF₆]

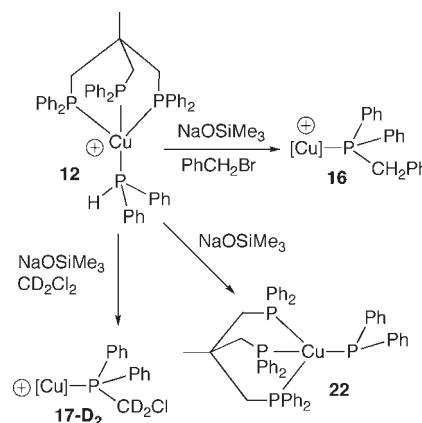
L	Cu–P(L)	Cu–P (triphos)	P–Cu–P(L)	P–Cu–P (triphos)
PH ₂ CH ₂ Fc (11)	2.2278(12)	2.2883(11) 2.2817(11) 2.2781(11)	118.36(4) 128.01(4) 119.15(4)	94.50(4) 92.00(4) 96.77(4)
PH ₂ Mes ^a	2.241(3)	2.279(3) 2.289(3) 2.262(3)	125.81(11) 119.50(10) 118.55(10)	94.6(1) 97.2(1) 94.13(9)
PHPh ₂ (12)	2.2262(9)	2.2692(9) 2.2776(9) 2.2804(9)	124.83(3) 120.47(3) 120.24(3)	96.58(3) 94.95(3) 92.28(3)
PHPh ₂ (12 -DFT)	2.3298	2.3913 (ave)	122.25 (ave)	94.16 (ave)
PHEt ₂ (13)	2.2466(7)	2.2817(6) 2.2866(6) 2.2922(6)	121.61(2) 127.32(2) 118.75(3)	93.92(2) 95.55(2) 91.66(2)
PHCy ₂ (14)	2.2531(6)	2.2914(6) 2.3040(6) 2.3367(6)	125.51(3) 122.13(2) 120.73(2)	95.35(2) 92.93(2) 91.72(2)
PPh ₂ CH ₂ Ph (16)	2.2648(11)	2.2971(11) 2.3041(10) 2.3296(10)	121.90(4) 127.92(4) 119.08(4)	93.25(4) 94.25(4) 91.92(4)
PPh ₂ CH ₂ Cl (17)	2.2642(13)	2.3085(14) 2.3130(14) 2.3093(12)	125.49(5) 120.10(5) 121.54(5)	91.78(4) 90.84(5) 99.53(5)
PPh ₃ ^b	2.2852(11)	2.2983(12) 2.3177(12) 2.3314(12)	122.79(4) 124.27(4) 117.67(4)	91.17(4) 96.58(4) 97.65(4)

^a Kourkine, I. V.; Maslennikov, S. V.; Ditchfield, R.; Glueck, D. S.; Yap, G. P. A.; Liable-Sands, L. M.; Rheingold, A. L. *Inorg. Chem.* **1996**, *35*, 6708–6716. ^b Yin, Q.; Gan, X. *Acta Crystallogr.* **2010**, *E66*, m369.

highly reactive. Attempts to observe such intermediates with dtbp or XantPhos ligands were unsuccessful. Treatment of [Cu(dtbp)(PHPh₂)(OTf)] (**20a**) with NaOSiMe₃ at –78 °C in THF-d₈ gave diphenylphosphine and dtbp, observed by ³¹P and ¹H NMR spectroscopy already at –70 °C. On warming to room temperature, the products were dtbp and a brick-red, insoluble precipitate, which is presumably the known [Cu(PPh₂)_n].²⁵ Consistent with this assignment, independently prepared [Cu(PPh₂)_n] did not react with dtbp under conditions in which the less sterically hindered N~N ligands bipy, phen, or neocuproine (2,9-Me₂phen) readily solubilized this oligomer to give dimeric or trimeric [Cu(N~N)(PPh₂)_n].⁹ Similarly, low-temperature reaction of NaOSiMe₃ with [Cu(XantPhos)(PHPh₂)] [PF₆] (**18**) gave XantPhos and several other unidentified P-containing compounds.

In contrast, we obtained evidence for the intermediate Cu(triphos)(PPh₂) (**22**) by trapping it with electrophiles and by direct NMR observation. Deprotonation of cationic PHPh₂ complex **12** in the presence of benzyl bromide gave diphenylbenzylphosphine complex **16**, while deprotonation of **12** in CD₂Cl₂ gave **17-D₂** containing a PPh₂CD₂Cl ligand (Scheme 8). These observations were consistent with the expected intermediacy of **22**, which was not observed under these conditions. However, generation of **22** in the absence of an electrophile was hindered by its limited solubility in nonpolar solvents. Therefore, soluble **12**-[B(Ar_F)₄] (Ar_F = 3,5-(CF₃)₂C₆H₃) was prepared by anion exchange. Its deprotonation at low temperature in THF-d₈ gave **22** (Scheme 8), which was readily identified by its ³¹P NMR spectrum (–50 °C, δ –23.4 (d, *J* = 27 Hz, triphos); –30.3 (q, *J* = 27 Hz, PPh₂); in Cu(PPh₃)(PPh₂) the phosphido group gave rise to a ³¹P NMR signal at δ –32.3 (d, *J* = 80 Hz; 30 °C, C₆D₆).²⁵ Intermediate **22** was also characterized by ¹H NMR spectroscopy.

Phosphido complex **22** underwent noticeable decomposition on warming to –30 °C and did not survive at room temperature; identifiable products included triphos and PHPh₂. To explore its high reactivity and nucleophilic behavior, intermediate **22** was characterized further, in

Scheme 8. Deprotonation of **12**: Formation of Cu-Phosphido Complex **22** and Its Reactions with Electrophiles^a

^a[Cu] = Cu(triphos). The anion for cations **12**, **16**, and **17-D₂** was PF₆; **22** was generated by deprotonation of **12**-B(Ar_F)₄.

comparison to precursor cation **12**, by DFT calculations (Table 4).

On deprotonation, both the Cu–P(PHPh₂) bond and the Cu–P(triphos) bonds lengthened slightly (for triphos, the average Cu–P bond length in cation **12** was 2.3913 Å; compare 2.4290 Å in **22**). This may reflect reduced electrostatic Cu–P attraction on conversion of cationic **12** to neutral **22**, the increased steric demands of the phosphido lone pair in comparison to the P–H group, or changes in hybridization at phosphorus.²⁶ While the P–Cu–P(L) angles showed greater variation in **22** than in **12**, their average value (124.37° (**22**)) did not change much from that in **12** (122.25°). In contrast, the P–Cu–P-(triphos) angles decreased slightly. The sum of angles at P in the phosphido complex was 322.2°; compare to 328.5° for an idealized tetrahedral geometry. This pyramidal structure is consistent with earlier observations on Pt and Re terminal phosphido complexes.²⁷

The nucleophilic nature of the M–X groups (X = OH, OR, SR, NR₂, PR₂) in complexes with late transition metal-heteroatom bonds has been ascribed either to

(24) An equilibrium between dimeric [Cu(dppe)(PPh₂)₂] and monomeric Cu(dppe)(PPh₂) was proposed on the basis of ebullioscopic molecular weight measurements: (a) Van Koten, G.; Noltes, J. G.; Spek, A. L. *J. Organomet. Chem.* **1978**, *159*, 441–463. (b) Greiser, T.; Weiss, E. *Chem. Ber.* **1978**, *111*, 516–522.

(25) Two-coordinate Cu(PPh₃)(PPh₂) was observed by ³¹P NMR spectroscopy: Lemmen, T. H.; Goeden, G. V.; Huffman, J. C.; Geerst, R. L.; Caulton, K. G. *Inorg. Chem.* **1990**, *29*, 3680–3685.

(26) (a) Deeming, A. J.; Doherty, S.; Marshall, J. E.; Powell, J. L.; Senior, A. M. *J. Chem. Soc., Dalton Trans.* **1993**, 1093–1100. (b) Zhuravel, M. A.; Glueck, D. S.; Zakharov, L. N.; Rheingold, A. L. *Organometallics* **2002**, *21*, 3208–3214. (c) Bonnet, G.; Kubicki, M. M.; Moise, C.; Lazzaroni, R.; Salvadori, P.; Vitulli, G. *Organometallics* **1992**, *11*, 964–967. (d) Reference 16a.

(27) (a) Mastrorilli, P. *Eur. J. Inorg. Chem.* **2008**, 4835–4850. (b) Eichenhofer, S.; Delacroix, O.; Kromm, K.; Gladysz, J. A. *Organometallics* **2005**, *24*, 245–255.

Table 4. Selected Bond Lengths (Å) and Angles (deg) in the Complexes [Cu(triphos)(L)]ⁿ⁺ (L = PPh₂, n = 1, **12**; L = PPh₂, n = 0, **22**), from DFT Calculations

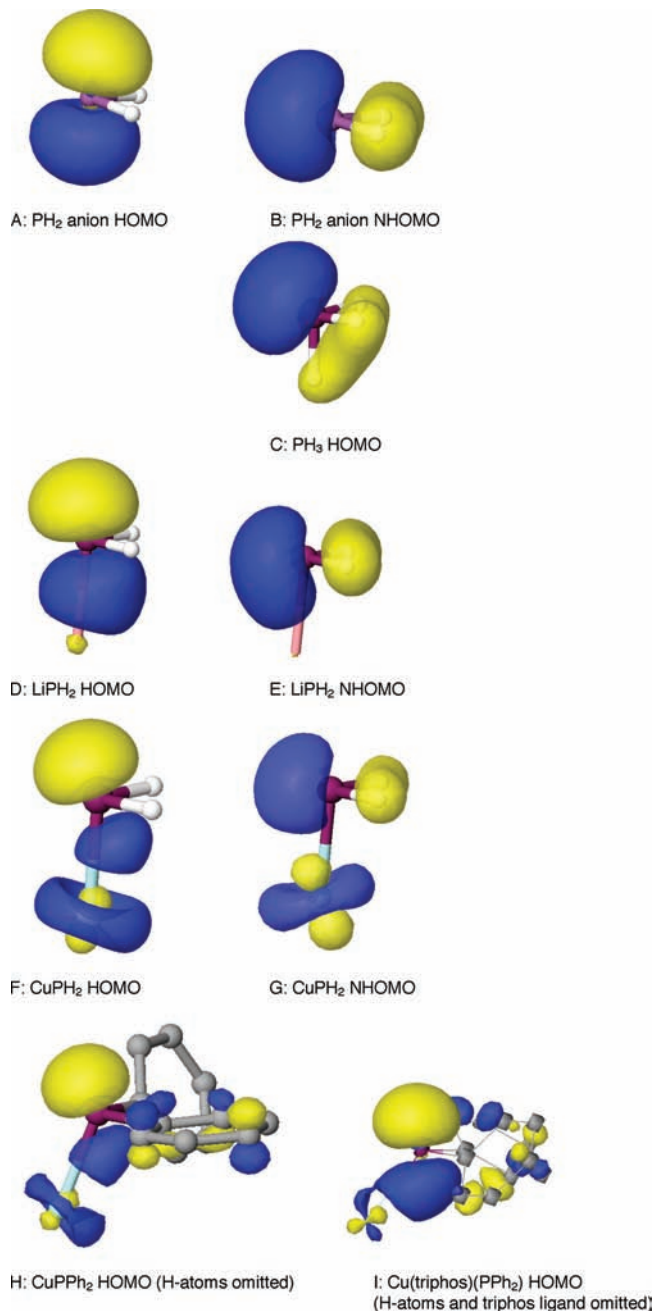
L	Cu–P(L)	Cu–P (triphos)	P–Cu–P(L)	P–Cu–P (triphos)
PPh ₂ (12)	2.3298	2.3911	122.21	94.00
		2.3909	120.06	94.01
		2.3918	124.48	94.47
PPh ₂ (22)	2.3374	2.4478	132.90	91.12
		2.4411	114.86	91.44
		2.3981	125.35	89.68

Table 5. Calculated Orbital Energies (eV) for Metal Phosphido Complexes and Phosphines

compound	P(p) HOMO energy	P(hybrid) NHOMO energy
Li(triphosH ₆)-PH ₂	−0.1360	−0.2152
Na(triphosH ₆)-PH ₂	−0.1335	−0.2135
K(triphosH ₆)-PH ₂	−0.1166	−0.2017
Cu(triphosH ₆)-PH ₂	−0.1589	−0.2108
Cu(triphos)-PPh ₂	−0.1419	−0.1983
PH ₂ anion	+0.0347	−0.0598
PPh ₂ anion	−0.0039	−0.0938
PPh ₂ -Li	−0.1668	−0.2433
PPh ₂ -Na	−0.1543	−0.2322
PPh ₂ -K	−0.1371	−0.2220
PPh ₂ -Cu	−0.2007	−0.2476
PH ₂ -Li	−0.1808	−0.2538
PH ₂ -Na	−0.1741	−0.2497
PH ₂ -K	−0.1445	−0.2281
PH ₂ -Cu	−0.2346	−0.2674
	P(hybrid) HOMO energy (eV)	
PH ₂ -H		−0.2801
PPh ₂ -H		−0.2354
PPh ₂ -CH ₂ Ph		−0.2257

repulsive π -symmetry interactions between filled metal orbitals and X lone pair orbitals, and/or to the ionic nature of the polarized $M^{\delta+}-X^{\delta-}$ bonds.^{28,6} We used DFT calculations on a series of phosphines and phosphido complexes to investigate the observed nucleophilicity of **22**. Alkali metal phosphido complexes were included to assess the effect of ionic bonding in cases where repulsive orbital interactions were not possible. Table 5 lists the calculated highest occupied molecular orbital (HOMO) and next highest occupied molecular orbital (NHOMO) energies.⁶

In the free PH₂[−] anion the HOMO is the b₂ p-orbital lying perpendicular to the molecular plane (Figure 10A), as expected, and the NHOMO is the a₁ MO lying in the molecular plane (Figure 10B); the NHOMO contains considerable s-character, making it lower in energy than the HOMO. When PH₂[−] is protonated to give a covalent P–H bond, the p-orbital is used to give a low lying σ -bonding MO, leaving the original PH₂[−] NHOMO as the new HOMO of the tertiary phosphine (Figure 10C). However, when a more electropositive element is used to make a metal-phosphido compound, the new bond formed using the PH₂[−] p-orbital has considerable ionic character, as shown for LiPH₂ in Figure 10D; while the energy of this molecular orbital (MO) is lowered relative to free PH₂[−] it is still high enough in energy to be the

**Figure 10.** DFT Kohn–Sham HOMOs and NHOMOs for phosphido anions and metal phosphido complexes.

HOMO of the phosphido complex, and as such is presumably responsible for the nucleophilic character of the metal-phosphido entity. As shown in Table 5, the energy of this HOMO is raised on changing the metal from Li to Na to K, in agreement with electronegativity ideas. For CuPH₂ the HOMO and NHOMO remain unchanged in nature (Figures 10F and 10G); compared to the alkali metal phosphides there is more covalency in the HOMO, as expected for the less electropositive Cu, but the HOMO is still higher in energy than that in PH₃. Adding triphosH₆ (triphosH₆ = MeC(CH₂PH₂)₃) ligands to the MPH₂ compounds raises the energy of the HOMO in each case, while not changing its overall character. Pictures of all the valence MOs of CuPH₂ are provided in the Supporting Information.

(28) (a) Caulton, K. G. *New J. Chem.* **1994**, *18*, 25–41. (b) Holland, P. L.; Andersen, R. A.; Bergman, R. G. *Comments Inorg. Chem.* **1999**, *21*, 115–129.

These observations carry through to CuPPh₂ (Figure 10H) and importantly also for Cu(triphos)(PPh₂) **22** (Figure 10I), in which the HOMO is still mostly phosphorus p in character, and considerably higher in energy than either PPh₂ or PPh₂CH₂Ph, consistent with their relative nucleophilicities.

Thus, the observed nucleophilicity of **22** could be explained in terms of a polarized Cu–P bond; the dominant contribution of the phosphorus p-orbital to the HOMO composition results from the relative electronegativities of these elements. In the alternative model, the HOMO of **22** is a σ^* -antibonding MO, whose increased energy results from filled–filled repulsive Cu–P orbital interactions. These computational results are similar to those for related Cu(I) anilido complexes, where the Kohn–Sham HOMOs were calculated to be primarily NHPp p - π orbitals, with minor π^* -character from mixing with a Cu d-orbital.²⁹

Ligand Substitution. The ligand substitution step required for catalytic turnover was observed on treatment of **16** or **17** with PPhPh₂ to yield equilibrium mixtures also containing **12** and the tertiary phosphines **4** or **7**; equilibrium constants for these reactions were about 8(2) and 7(2) respectively, favoring complexation of the smaller secondary phosphine (Scheme 9). These reactions occurred on mixing and reached equilibrium within minutes; identical results were obtained starting from **12**.³⁰

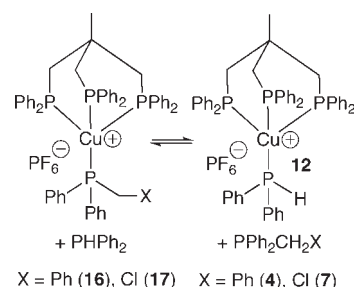
Conclusions

These observations are consistent with a proposed mechanism for catalytic P–C bond formation, involving deprotonation of the cationic diphenylphosphine complex [Cu(triphos)-(PPhPh₂)]PF₆ (**12**) by NaOSiMe₃ to yield the phosphido complex Cu(triphos)(PPh₂) (**22**). Nucleophilic attack on the substrate (benzyl halide or CH₂Cl₂) then yields the tertiary phosphine complex [Cu(triphos)(PPh₂CH₂X)]PF₆ (X = Ph (**16**) or Cl (**17**)), and ligand substitution with PPhPh₂ regenerates **12** (Scheme 10).

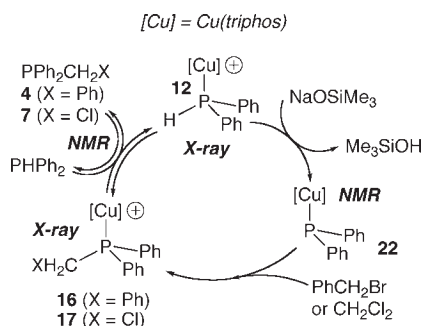
This proposed mechanism is related to those suggested for catalytic C–X (X = N, O, S) bond formation mediated by nucleophilic Cu(I) amide, alkoxide, and thiolate complexes.^{31,6} In contrast, Cu-catalyzed aryl amination and etherification may proceed via Cu(I)/Cu(III) cycles or other processes involving electron transfer,³² while little is known about the mechanism of Cu-catalyzed phosphination of aryl halides.³³

Development of the copper-catalyzed alkylations of diphenylphosphine reported here exploited the anticipated nucleophilicity of a Cu(I) terminal phosphido intermediate and rapid ligand substitution at the labile copper center. The

Scheme 9. Ligand Substitution in Cationic Cu(triphos) Complexes



Scheme 10. Proposed Mechanism for Cu(triphos)-Catalyzed Alkylation of Diphenylphosphine



observed dissociation of bidentate XantPhos and dtbp ligands confirmed our fears that this lability could be a problem. However, Cu catalysts containing tridentate triphos were more robust and enabled a new reaction, catalytic phosphination of methylene chloride. In future work, we plan to investigate the scope and limitations of such P–C bond-forming reactions, and to develop related asymmetric catalysis using chiral analogues of triphos.³⁴

Experimental Section

General Experimental Details. Unless otherwise noted, all reactions and manipulations were performed in dry glassware under a nitrogen atmosphere at ambient temperature in a dry-box or using standard Schlenk techniques. Petroleum ether (bp 38–53 °C), CH₂Cl₂, ether, THF, and toluene were dried over alumina columns similar to those described by Grubbs.³⁵ NMR spectra were recorded by using a Varian 300 or 500 MHz spectrometer. ¹H or ¹³C NMR chemical shifts are reported versus Me₄Si and were determined by reference to the residual ¹H or ¹³C solvent peaks. ³¹P NMR chemical shifts are reported versus H₃PO₄ (85%) used as an external reference. Coupling constants are reported in hertz (Hz), as absolute values unless noted otherwise. Unless indicated, peaks in NMR spectra are singlets. IR spectra were recorded on KBr disks and are reported in cm⁻¹. Quantitative Technologies Incorporated provided elemental analyses. Mass spectrometry was performed at the University of Illinois. Unless otherwise noted, reagents were from commercial suppliers; these compounds were prepared by the literature methods: [Cu(NCMe)₄][PF₆] (**1**),³⁶ Ph₂CH₂Fc,³⁷ PPhMe(Is),³⁸ Cu(dtbp)(Cl) (**5**) and Cu(dtbp)(OTf) (**6**),¹⁴ and [K][B(AR_F)₄].³⁹

(34) (a) Burk, M. J.; Harlow, R. L. *Angew. Chem., Int. Ed.* **1990**, *29*, 1462–1464. (b) Burk, M. J.; Feaster, J. E.; Harlow, R. L. *Tetrahedron: Asymmetry* **1991**, *2*, 569–592. (c) Ward, T. R.; Venanzi, L. M.; Albinati, A.; Lianza, F.; Gerfin, T.; Gramlich, V.; Ramos Tombo, G. M. *Helv. Chim. Acta* **1991**, *74*, 983–988.

(35) Pangborn, A. B.; Giardello, M. A.; Grubbs, R. H.; Rosen, R. K.; Timmers, F. J. *Organometallics* **1996**, *15*, 1518–1520.

(36) Kubas, G. J. *Inorg. Synth.* **1990**, *28*, 68–70.

(29) Goj, L. A.; Blue, E. D.; Delp, S. A.; Gunnoe, T. B.; Cundari, T. R.; Pierpont, A. W.; Petersen, J. L.; Boyle, P. D. *Inorg. Chem.* **2006**, *45*, 9032–9045.

(30) On treatment of [Cu(XantPhos)(PPh₂CH₂Ph)]PF₆ (**19**) with PPhPh₂, the ³¹P NMR spectrum (CD₂Cl₂, 21 °C) was consistent with rapid ligand substitution on the NMR time scale. Three broad peaks (δ –4.7, –10.2, –24.7), assigned to PPh₂CH₂Ph, XantPhos, and PPhPh₂, respectively, were observed.

(31) Gunnoe, T. B. *Eur. J. Inorg. Chem.* **2007**, 1185–1203.

(32) (a) Jones, G. O.; Liu, P.; Houk, K. N.; Buchwald, S. L. *J. Am. Chem. Soc.* **2010**, *132*, 6205–6213. (b) References 21b, 21c.

(33) (a) Gelman, D.; Jiang, L.; Buchwald, S. L. *Org. Lett.* **2003**, *5*, 2315–2318. (b) Van Allen, D.; Venkataraman, D. *J. Org. Chem.* **2003**, *68*, 4590–4593. (c) Tani, K.; Behenna, D. C.; McFadden, R. M.; Stoltz, B. M. *Org. Lett.* **2007**, *9*, 2529–2531. (d) Huang, C.; Tang, X.; Fu, H.; Jiang, Y.; Zhao, Y. *J. Org. Chem.* **2006**, *71*, 5020–5022.

[Cu(triphos)(NCMe)][PF₆] (2). A white slurry of [Cu(NCMe)₄][PF₆] (1; 250 mg, 0.671 mmol) in 5 mL of THF was treated with a solution of triphos (419 mg, 0.671 mmol) in 2 mL of THF and rapidly stirred overnight. The reaction mixture became somewhat more clear and homogeneous, but still contained an off-white tint. It was pumped down under vacuum. The residue was washed with petroleum ether and then recrystallized from methylene chloride layered with petroleum ether at -30 °C to give a white solid (585 mg, 0.670 mmol, 99.8%). Crystals suitable for elemental analysis and X-ray crystallography were obtained by dissolving the white solid in a minimal amount of methylene chloride followed by diffusion of petroleum ether vapors at -30 °C. Scale-up: Starting with 1.789 g of [Cu(NCMe)₄][PF₆] gave 3.947 g of [Cu(triphos)(NCMe)][PF₆] (94% yield).

Anal. Calcd. for C₄₃H₄₂P₄NF₆Cu: C, 59.08; H, 4.84; N, 1.60. Found: C, 58.83; H, 4.89; N, 1.56. HRMS *m/z* calcd for C₄₁H₃₉P₃Cu (M-NCMe)⁺: 687.1561. Found: 687.1561. ³¹P{¹H} NMR (CD₂Cl₂): δ -20.6 (broad), -143.4 (septet, *J* = 711). ¹H NMR (CD₂Cl₂): δ 7.36 (br, 12H, Ar), 7.24 (t, *J* = 8, 6H, Ar), 7.15 (t, *J* = 8, 12H, Ar), 2.69 (br, 3H, CH₃), 2.49 (br, 6H, CH₂), 1.62 (br, 3H, CH₃). ¹³C{¹H} NMR (CD₂Cl₂): δ 134.7 (m, Ar), 131.9 (m, Ar), 130.2 (Ar), 129.0 (m, Ar), 122.6 (NC), 39.1 (m, CH₃), 36.4 (br, MeC), 35.7 (br, CH₂), 3.7 (NCCH₃). ¹⁹F{¹H} NMR (CD₂Cl₂): δ -73.5 (d, *J* = 711).

[Cu(XantPhos)(NCMe)][PF₆] (3). A slurry of [Cu(NCMe)₄][PF₆] (1; 150 mg, 0.403 mmol) in 5 mL of THF was treated with a slurry of XantPhos (233 mg, 0.403 mmol) in 5 mL of THF and stirred for 2 h. The reaction mixture became homogeneous and was pumped down under vacuum. The residue was washed with petroleum ether (2 × 10 mL) and dried under vacuum. The crude product was then dissolved in CH₂Cl₂, filtered through Celite, and the resulting solution was layered with petroleum ether and cooled to -30 °C yielding a white crystalline solid (280 mg, 0.338 mmol, 84%). Crystals suitable for elemental analysis and X-ray crystallography were obtained by slow diffusion of petroleum ether vapors into a methylene chloride solution at -30 °C. Scale-up: 300 mg of [Cu(NCMe)₄][PF₆] gave 629 mg of [Cu(XantPhos)(NCMe)][PF₆] (94% yield).

Anal. Calcd. for C₄₁H₃₅CuNOP₃F₆: C, 59.46; H, 4.26; N, 1.69. Found: C, 59.05; H, 4.28; N, 1.62. HRMS *m/z* calcd for C₃₉H₃₂CuOP₂ (M-NCMe)⁺: 641.1224. Found: 641.1237. ³¹P{¹H} NMR (CD₂Cl₂): δ -13.0 (XantPhos), -143.5 (septet, *J* = 711, PF₆). ¹H NMR (CD₂Cl₂): δ 7.68 (dd, *J* = 2, 8, 2H, Ph), 7.46 (t, *J* = 7, 4H, Ph), 7.36 (t, *J* = 8, 8H, Ph), 7.31-7.27 (m, 8H, Ph), 7.23 (t, *J* = 8, 2H, Ph), 6.72 (br m, 2H, Ph), 2.23 (3H, NCMe), 1.71 (6H, Me). ¹³C{¹H} NMR (CD₂Cl₂): δ 154.5 (t, *J* = 6, Ph), 133.7 (t, *J* = 2, Ph), 133.5 (t, *J* = 8, Ph), 131.8 (Ph), 130.8 (Ph), 130.2 (t, *J* = 19, Ph), 129.3 (t, *J* = 5, Ph), 128.1 (Ph), 125.4 (t, *J* = 2, Ph), 120.7 (Ph), 118.7 (t, *J* = 16, NCMe), 36.0 (CMe₂), 28.5 (Me), 2.5 (NCMe).

Cu-Catalyzed Alkylation of PPh₂ with PhCH₂X (X = Br, Cl); Synthesis of PPh₂CH₂Ph (4; Entries 2 and 3, Table 2). [Cu(triphos)(NCMe)][PF₆] (2; 23 mg, 0.027 mmol (10 mol %) or 2.3 mg, 0.0027 mmol (1 mol %)) was dissolved in a few drops of CH₂Cl₂ and treated with a solution of PPh₂ (50 mg, 0.27 mmol) in 1 mL of CH₂Cl₂, then with dry, degassed benzyl bromide (32 μL, 0.27 mmol). This mixture was added to a rapidly stirring slurry of NaOSiMe₃ (30 mg, 0.27 mmol) in 1 mL of CH₂Cl₂. The reaction, monitored by ³¹P NMR spectroscopy, was complete in less than 10 min, but was likely faster; a large amount of precipitate formed within 1 min. The reaction mixture was pumped down

under vacuum. The residue was dissolved in 10 mL of a 10% THF/petroleum ether solution. The solution was passed through a silica plug, and the filtrate was pumped down under vacuum to yield a white solid (61 mg, 0.22 mmol, 82%). In the experiment with 1 mol % catalyst loading, the reaction was complete after 2 h; 20% THF/petroleum ether was used for workup, and the yield was 87%. A similar procedure was used for the other entries in Table 2 involving benzyl bromide and chloride (entries 1 and 4-17); see the Supporting Information for details.

Cu-Catalyzed Alkylation of CH₂Cl₂; Synthesis of PPh₂CH₂Cl (7; Table 2, Entry 18). A solution of [Cu(triphos)(NCMe)][PF₆] (2; 23 mg, 0.027 mmol, 10 mol %) and PPh₂ (50 mg, 0.27 mmol) in 2 mL of CH₂Cl₂ was added to a stirring solution of NaOSiMe₃ (30 mg, 0.27 mmol) in 1 mL of CH₂Cl₂, resulting in a flash of yellow color, which dissipated within a minute. After 25 min, all of the PPh₂ had been consumed, according to ³¹P NMR monitoring. The solution was pumped down under vacuum, the residue was dissolved in 10 mL of 10% THF/petroleum ether, and this solution was passed through a silica plug. The filtrate was pumped down, giving a clear oil (54 mg, 0.23 mmol, 86%). NMR data for 7 matched literature reports.¹⁵ ³¹P{¹H} NMR (CDCl₃): δ -7.9. ¹H NMR (CDCl₃): 7.52-7.49 (m, 4H, Ph), 7.42-7.40 (m, 6H, Ph), 4.08 (d, *J* = 5, 2H, CH₂). ¹³C{¹H} NMR (CDCl₃): 135.6 (d, *J* = 12, Ph), 133.2 (d, *J* = 19, Ph), 129.6 (Ph), 128.9 (d, *J* = 7, Ph), 41.0 (d, *J* = 27, CH₂).

Cu-Catalyzed Alkylation of PPh₂ with PhCHMe(Br); Synthesis of PPh₂CHMe(Ph) (8; Table 2, Entry 20). A solution of (1-bromoethyl)benzene (37 μL, 0.27 mmol) in 1 mL of THF was added to a stirred slurry of [Cu(triphos)(NCMe)][PF₆] (2; 23 mg, 0.027 mmol) and PPh₂ (50 mg, 0.27 mmol) in 2 mL of THF. A solution of NaOSiMe₃ (30 mg, 0.27 mmol) in 2 mL of THF was added with stirring, resulting in a bright yellow solution, which became milky white as precipitation occurred within minutes. After 15 min, ³¹P NMR spectroscopy revealed full conversion to a 33:1 mixture of PPh₂CH(Me)Ph (8) and Ph₂P-PPh₂ (9). The reaction mixture was pumped down under vacuum and the residue was extracted with a 10% THF/petroleum ether solution. The extract was passed through a silica plug, and the filtrate was pumped down, giving oily, white solid 8 (79 mg, 0.27 mmol, 100%) in 97% purity by ³¹P NMR spectroscopy. The identity of the impurity (9) was confirmed by spiking the product with Ph₂P-PPh₂ (Aldrich).

NMR spectra for 8 matched literature data.¹⁷ ³¹P{¹H} NMR (CDCl₃): δ 3.6 (97%, PhCHMePPh₂), -13.9 (3%, Ph₂P-PPh₂). ¹H NMR (CDCl₃): δ 7.68-7.65 (m, 2H, Ph), 7.45-7.42 (m, 3H, Ph), 7.24-7.10 (m, 10H, Ph), 3.57 (apparent quintet, *J* = 7.5, 1H, CH), 1.45 (m, 3H, CH₃).

Cu-Catalyzed Reaction of PPh₂ with Dibromoethane; Synthesis of Ph₂P-PPh₂ (9; Table 2, Entry 26). An NMR tube was charged with a solution of [Cu(triphos)(NCMe)][PF₆] (2; 23 mg, 0.027 mmol) in a few drops of CH₂Cl₂, a solution of PPh₂ (50 mg, 0.27 mmol) in 1 mL of CH₂Cl₂, and 1,2-dibromoethane (12 μL, 0.13 mmol). This mixture was added to a stirred slurry of NaOSiMe₃ (30 mg, 0.27 mmol) in 1 mL of CH₂Cl₂, and the catalysis was monitored by ³¹P NMR spectroscopy. After 15 min, the reaction was complete, yielding Ph₂P-PPh₂ (9) and a small amount of its oxide, Ph₂P-PPh₂(O);⁴⁰ no Ph₂PCH₂Cl was formed. The reaction mixture was pumped down under vacuum. The residue was dissolved in 10 mL of a 10% THF/petroleum ether solution and passed through a silica plug. The resulting solution was pumped down under vacuum affording a white solid (35 mg, 0.095 mmol, 71%), which contained Ph₂P-PPh₂ and a trace of Ph₂P-P(O)Ph₂, as observed by ³¹P NMR spectroscopy. The formation of 9 was confirmed by ³¹P and ¹H

(37) (a) Pet, M. A.; Cain, M. F.; Hughes, R. P.; Glueck, D. S.; Golen, J. A.; Rheingold, A. L. *J. Organomet. Chem.* **2009**, *694*, 2279-2289. (b) Goodwin, N. J.; Henderson, W.; Nicholson, B. K. *Chem. Commun.* **1997**, 31-32.

(38) Brauer, D. J.; Bitterer, F.; Dorrenbach, F.; Hessler, G.; Stelzer, O.; Kruger, C.; Lutz, F. Z. *Naturforsch. B* **1996**, *51*, 1183-1196.

(39) Brookhart, M.; Grant, B.; Volpe, A. F., Jr. *Organometallics* **1992**, *11*, 3920-3922.

(40) Irvine, D. J.; Glidewell, C.; Cole-Hamilton, D. J.; Barnes, J. C.; Howie, A. *J. Chem. Soc., Dalton Trans.* **1991**, 1765-1772.

NMR after spiking this material with an authentic sample of $\text{Ph}_2\text{P-PPH}_2$ (Aldrich).

[Cu(triphos)(PH_2Ph)][PF_6] (10). A stirring white slurry of [Cu(triphos)(NCMe)][PF_6] (**2**; 50 mg, 0.057 mmol) in 5 mL of THF was treated with a solution of PH_2Ph (6.3 mg, 0.057 mmol) in 1 mL of THF resulting in a homogeneous solution with a pink tint. The mixture was stirred for 3 h; it became significantly darker. The reaction mixture was pumped down, and the residue was washed with petroleum ether. The crude product was recrystallized from methylene chloride layered with petroleum ether at -30°C to give a flaky gray-pink solid (52 mg, 0.055 mmol, 96%). White crystals suitable for elemental analysis were obtained by dissolving the solid in THF followed by diffusion of petroleum ether vapors at -30°C . Scaleup: 200 mg of **2** gave the product in quantitative yield.

Anal. Calcd. for $\text{C}_{47}\text{H}_{46}\text{CuF}_6\text{P}_5$: C, 59.85; H, 4.92. Found: C, 59.76; H, 4.97. HRMS m/z calcd for $\text{C}_{47}\text{H}_{47}\text{CuP}_4$ (MH^+): 798.1924. Found: 798.1965. $^{31}\text{P}\{^1\text{H}\}$ NMR (CD_2Cl_2): δ -16.4 (broad), -91.0 (very broad), -143.5 (septet, $J = 711$). ^1H NMR (CD_2Cl_2): δ 7.76 (m, 2H, Ar), 7.58 (t, $J = 8$, 1H, Ar), 7.47 (m, 2H, Ar), 7.25 (t, $J = 7$, 6H, Ar), 7.13 (broad, 12H, Ar), 7.08 (t, $J = 8$, 12H, Ar), 5.98 (dq, $J = 9$, 313, 2H, PH_2), 2.57 (broad, 6H, CH_2), 1.69 (q, $J = 3$, 3H, CH_3). $^{13}\text{C}\{^1\text{H}\}$ NMR (CD_2Cl_2): δ 133.9 (m, Ar), 133.6 (d, $J = 13$, P-Ar), 131.8 (q, $J = 5$, Ar), 130.8 (d, $J = 1$, P-Ar), 130.4 (Ar), 129.8 (d, $J = 10$, P-Ar), 129.1 (q, $J = 3$, Ar), 123.9 (dq, $J = 4$, 38, P-Ar), 39.0 (q, $J = 11$, CH_3), 36.2 (m, CH_3C), 35.9 (m, CH_2). IR (Nujol): 2919, 2324 (P-H stretch), 1964, 1585, 1573, 1418, 1378, 1332, 1306, 1095, 1072, 1025, 999 cm^{-1} .

[Cu(triphos)($\text{PH}_2\text{CH}_2\text{Fc}$)][PF_6] (11). A white slurry of [Cu(triphos)(NCMe)][PF_6] (**2**; 50 mg, 0.057 mmol) was stirred in 5 mL of THF and treated with a yellow solution of FcCH_2PH_2 (13.3 mg, 0.057 mmol) in less than 1 mL of THF; the mixture became yellow-orange and homogeneous. After stirring overnight, the reaction mixture was pumped down, and the residue was washed with petroleum ether. The crude product was then recrystallized from methylene chloride layered with petroleum ether at -30°C to give a golden brown solid (61 mg, 0.057 mmol, 100%). X-ray quality crystals were grown by dissolving the solid in warm methanol and allowing it to slowly cool at -30°C . Scaleup: 200 mg of **2** gave the product in quantitative yield.

Anal. Calcd. for $\text{C}_{52}\text{H}_{52}\text{CuF}_6\text{FeP}_5$: C, 58.63; H, 4.92. Analyses were consistently low in carbon, for example: Found: C, 57.97; H, 4.79. HRMS m/z calcd for $\text{C}_{52}\text{H}_{53}\text{P}_4\text{CuFe}$ (MH^+): 920.1743. Found: 920.1766. $^{31}\text{P}\{^1\text{H}\}$ NMR (CD_2Cl_2): δ -16.6 (broad), -94.3 (very broad), -143.5 (septet, $J = 711$). ^1H NMR (CD_2Cl_2): δ 7.26 (t, $J = 7$, 6H, Ar), 7.17 (br, 12H, Ar), 7.12 (t, $J = 7$, 12H, Ar), 4.92 (dq, $J = 8$, 305, 2H, PH_2), 4.32 (br, 2H, Fc), 4.22 (br, 7H, Fc), 3.33 (br, 2H, PCH_2Fc), 2.52 (br, 6H, CH_2), 1.66 (br, 3H, CH_3). $^{13}\text{C}\{^1\text{H}\}$ NMR (CD_2Cl_2): δ 134.1 (m, Ar), 131.8 (m, Ar), 130.4 (Ar), 129.2 (m, Ar), 85.0 (Fc), 69.4 (Fc), 68.71-68.67 (m, Fc), 39.0 (apparent quartet, $J = 11$, CH_3), 36.1 (m, C-CH_3), 35.7 (m, MeC-CH_2), 19.9 (dq, $J = 5$, 18, $\text{P-CH}_2\text{Fc}$). IR (Nujol): 2902, 2728, 2329 (P-H stretch), 1481, 1435, 1378, 1104, 1095, 1025, 999, 923, 875, 736 cm^{-1} .

[Cu(triphos)(PHPh_2)][PF_6] (12). A white slurry of [Cu(triphos)(NCMe)][PF_6] (**2**; 50 mg, 0.057 mmol) was stirred in 5 mL of THF and treated with a solution of PHPh_2 (10.7 mg, 0.057 mmol) in 1 mL of THF to give a clear solution. The mixture was stirred overnight and was cloudy by morning. The solvent was pumped down, and the residue was washed with petroleum ether. The crude product was recrystallized from methylene chloride layered with petroleum ether at -30°C to give a white precipitate (56 mg, 0.055 mmol, 97%). X-ray quality crystals were obtained by dissolving the white solid in a minimal amount of methylene chloride followed by diffusion of petroleum ether vapors at -30°C . Scale-up: 1.0 g of [Cu(triphos)(NCMe)][PF_6] gave [Cu(triphos)(PHPh_2)][PF_6] in quantitative yield.

Anal. Calcd. for $\text{C}_{53}\text{H}_{50}\text{CuF}_6\text{P}_5 \cdot 1.2\text{CH}_2\text{Cl}_2$: C, 58.06; H, 4.71. Found: C, 57.51; H, 4.75. One equivalent of CH_2Cl_2 per copper complex was observed by X-ray crystallography. Integration of this sample's ^1H NMR spectrum indicated the presence of 1.2 molecules of CH_2Cl_2 . HRMS m/z calcd for $\text{C}_{53}\text{H}_{50}\text{CuP}_4$ (M^+): 873.2160. Found: 873.2160. $^{31}\text{P}\{^1\text{H}\}$ NMR (CD_2Cl_2): δ -16.2 (broad), -143.5 (septet, $J = 711$). $^{31}\text{P}\{^1\text{H}\}$ NMR (CD_2Cl_2 , -70°C): -16.0 (broad, triphos), -19.4 (broad, PHPh_2), -143.7 (septet, $J = 711$, PF_6). ^1H NMR (CD_2Cl_2): δ 7.71 (t, $J = 7$, 4H, Ar), 7.56 (t, $J = 7$, 2H, Ar), 7.41 (t, $J = 7$, 4H, Ar), 7.25 (m, 6H, Ar), 7.04 (br, 24H, Ar), overlapping 6.99 (dq, $J = 381$, 7, 1H, PH), 2.61 (br, 6H, CH_2), 1.70 (br, 3H, CH_3). $^{13}\text{C}\{^1\text{H}\}$ NMR (CD_2Cl_2): δ 134.1 (m, Ar), 133.5 (d, $J = 13$, P-Ar), 131.9 (q, $J = 5$, Ar), 131.1 (d, $J = 1$, P-Ar), 130.6 (m, P-Ar), 130.3 (Ar), 129.7 (d, $J = 9$, P-Ar), 129.1 (q, $J = 3$, Ar), 39.1 (q, $J = 11$, CH_3), 36.2 (broad, overlapping $\text{CH}_3\text{C-CH}_2$). IR (Nujol): 2917, 2726, 1963, 1483, 1480, 1465, 1434, 1378, 1095, 876, 835, 761, 736, 700, 557 cm^{-1} .

[Cu(triphos)(PHEt_2)][PF_6] (13). A white slurry of [Cu(triphos)(NCMe)][PF_6] (**2**; 50 mg, 0.057 mmol) was stirred in 5 mL of THF and treated with a solution of PHEt_2 (5.2 mg, 0.057 mmol) in 1 mL of THF to give a clear solution. The mixture was stirred for 4 h, pumped down under vacuum, and the residue was washed with petroleum ether. The crude product was recrystallized from methylene chloride layered with petroleum ether at -30°C to give an off-white/beige solid (53 mg, 0.057 mmol, 100%). Crystals suitable for X-ray and elemental analyses were obtained by dissolving this material in a minimal amount of methylene chloride followed by diffusion of petroleum ether vapors at -30°C . Scaleup: 200 mg of **2** gave the product in quantitative yield.

Anal. Calcd. for $\text{C}_{45}\text{H}_{50}\text{CuF}_6\text{P}_5$: C, 58.54; H, 5.46. Found: C, 58.13; H, 5.70. HRMS m/z calcd for $\text{C}_{45}\text{H}_{51}\text{CuP}_4$ (MH^+): 778.2237. Found: 778.2274. $^{31}\text{P}\{^1\text{H}\}$ NMR (CD_2Cl_2): δ -16.7 (broad), -33.4 (broad), -143.5 (septet, $J = 711$). ^1H NMR (CD_2Cl_2): δ 7.27 (t, $J = 7$, 6H, Ar), 7.15-7.11 (br, 24H, Ar), 4.85 (dm, $J = 300$, 1H, PH), 2.55 (6H, CH_2), 2.17 (m, 4H, PHCH_2), 1.67 (q, $J = 3$, 3H, CH_3), 1.36 (dt, $J = 16$, 8, 6H, CH_3). $^{13}\text{C}\{^1\text{H}\}$ NMR (CD_2Cl_2): δ 134.6 (m, Ar), 131.8 (q, $J = 5$, Ar), 130.3 (Ar), 129.1 (q, $J = 3$, Ar), 39.0 (m, CH_3), 36.3 (m, CH_3C), 36.0 (m, CH_2), 15.3 (dq, $J = 4$, 17, P-CH_2), 11.6 (d, $J = 2$, PCH_2CH_3). IR (Nujol): 3059, 2728, 2674, 2301 (P-H stretch), 1572, 1482, 1416, 1403, 1400, 1378, 1333, 1310, 1276, 1267, 1184, 1166, 1161, 1157, 1147, 1096, 1073, 1041, 1027, 1001, 970, 958, 922 cm^{-1} .

[Cu(triphos)(PHCy_2)][PF_6] (14). A white slurry of [Cu(triphos)(NCMe)][PF_6] (**2**; 50 mg, 0.057 mmol) in 5 mL of THF was treated with a solution of PHCy_2 (11.3 mg, 0.057 mmol) in 2 mL of THF to give a clear solution. The mixture was stirred for 5 h and pumped down under vacuum. The residue was washed with petroleum ether (2×10 mL) and dried under vacuum. The crude product was recrystallized from CH_2Cl_2 layered with petroleum ether at -30°C to give a white solid (56 mg, 0.054 mmol, 95%). Crystals suitable for X-ray and elemental analysis were obtained by dissolving the solid in THF followed by diffusion of petroleum ether vapors at -30°C . Scaleup: 200 mg of **2** gave a quantitative yield of the product.

Anal. Calcd. for $\text{C}_{53}\text{H}_{62}\text{CuF}_6\text{P}_5 \cdot 0.5\text{THF}$: C, 61.98; H, 6.37. Found: C, 62.35; H, 6.32. One equivalent of THF per copper complex was observed by X-ray crystallography. Before elemental analysis, a sample was placed under vacuum; ^1H NMR integration then showed that 0.5 equiv of THF remained. HRMS m/z calcd for $\text{C}_{53}\text{H}_{63}\text{CuP}_4$ (MH^+): 886.3176. Found: 886.3135. $^{31}\text{P}\{^1\text{H}\}$ NMR (CD_2Cl_2): δ -7.7 (broad), -18.2 (broad), -143.5 (septet, $J = 711$). ^1H NMR (CD_2Cl_2): δ 7.31 (t, $J = 7$, 6H, Ar), 7.15-7.10 (broad, 24H, Ar), 4.53 (dm, $J = 293$, 1H, PH), 2.59 (br, 6H, CH_2), 2.20 (m, 2H, Cy), 1.98 (m, 4H, Cy), 1.73-1.61 (overlapping m, 3H Me + 6H Cy), 1.37 (m, 5H, Cy), 1.25 (m, 5H, Cy). $^{13}\text{C}\{^1\text{H}\}$ NMR (CD_2Cl_2): δ 134.6 (m, Ar), 132.1 (q, $J = 5$, Ar), 130.3 (Ar), 129.1 (q, $J = 3$, Ar), 39.1 (q, $J = 10$, C-CH_3), 36.7 (br d, $J = 4$, C-CH_3), 35.9 (m, $\text{CH}_3\text{C-CH}_2$),

32.6 (d, $J = 4$, Cy), 31.9 (d, $J = 3$, Cy), 31.8 (Cy), 27.0 (d, $J = 10$, Cy), 26.8 (d, $J = 12$, Cy), 25.6 (Cy). IR (Nujol): 3052, 2728, 2670, 2314 (P–H stretch), 1585, 1573, 1483, 1462, 1450, 1418, 1403, 1378, 1334, 1310, 1269, 1229, 1183, 1173, 1160, 1096, 1073, 1043, 1026, 1000, 964, 916, 875, 734 cm^{-1} .

[Cu(triphos)(PHMe(Is))][PF₆] (15). A white slurry of [Cu(triphos)(NCMe)][PF₆] (**2**; 200 mg, 0.23 mmol) in 5 mL of THF was treated with a solution of PHMe(Is) (58 mg, 0.23 mmol) in 2 mL of THF, resulting in a clear solution. The mixture was stirred for 3 h, pumped down under vacuum, and washed with petroleum ether (2 × 10 mL). The crude product was recrystallized from methylene chloride layered with petroleum ether at –30 °C to give a white solid (243 mg, 0.22 mmol, 98%). Crystals suitable for elemental analysis were obtained from a second recrystallization from CH₂Cl₂/petroleum ether at –30 °C.

Anal. Calcd. for C₅₇H₆₆CuP₅F₆: C, 63.18; H, 6.14. Found: C, 62.95; H, 5.73. HRMS m/z calcd for C₅₇H₆₆CuP₄ (M⁺): 937.3412. Found: 937.3411. ³¹P{¹H} NMR (CD₂Cl₂): δ –17.8 (broad, triphos), –81.6 (broad, PHMe(Is)), –143.5 (septet, $J = 711$, PF₆). ¹H NMR (CDCl₃): δ 7.22–7.20 (m, 6H, Ph), 7.17 (br, 2H, Ph), 7.12 (br, 12H, Ph), 7.04–7.00 (br m, 12H, Ph), 6.38 (dm, $J = 313$, 1H, PH), 3.49 (br, 2H, CH), 2.97 (septet, $J = 7$, 1H, CH), 2.49 (br, 6H, CH₂), 2.07 (m, 3H, PHMe), 1.62 (br, 3H, CH₃), 1.33–1.28 (br m, 18H, CH₃(Is)). ¹³C{¹H} NMR (CD₂Cl₂): δ 151.9 (Ar), 134.5 (m, Ar), 132.0 (m, Ar), 130.4 (Ar), 129.2 (m, Ar), 124.8 (dm, $J = 32$, Ar), 122.9 (br, Ar), 39.1 (m, CH₃), 36.4 (br, MeC), 35.9 (m, CH₂), 34.6 (*i*-Pr), 33.4 (br, *i*-Pr), 25.0 (br, *i*-Pr), 23.9 (d, $J = 3$, *i*-Pr), 12.5 (dm, $J = 16$, P-Me). IR (Nujol): 2953, 2923, 2854, 2397 (P–H stretch), 1463, 836, 694 cm^{-1} .

[Cu(triphos)(PPh₂CH₂Ph)][PF₆] (16). A slurry of [Cu(triphos)(NCMe)][PF₆] (**2**; 100 mg, 0.114 mmol) in 5 mL of THF was treated with a solution of benzylidiphenylphosphine (**4**; 32 mg, 0.11 mmol) in 1 mL of THF and rapidly stirred. Within 1 min, the solution became clear and homogeneous, but it was stirred for 1 h to ensure complete conversion. The reaction mixture was pumped down and washed with petroleum ether (2 × 10 mL). The residue was recrystallized from methylene chloride layered with petroleum ether at –30 °C to give a white, fluffy solid (130 mg, 0.114 mmol, 100%). Crystals suitable for X-ray analysis were obtained by diffusion of petroleum ether vapors into a solution of **16** in CH₂Cl₂ over the course of several days at –30 °C, leading to the formation of a large white crystal. When the solution was pipetted away from the crystal, it desolvated, but when the solution was transferred to a separate vial, it suddenly formed several white snowflake-like crystals of X-ray quality.

Anal. Calcd. for C₆₀H₅₆CuP₃F₆: C, 64.95; H, 5.09. Found: C, 64.49; H, 4.84. HRMS m/z calcd for C₆₀H₅₆CuP₄ (M⁺): 963.2629. Found: 963.2604. ³¹P{¹H} NMR (CD₂Cl₂): δ 9.2 (PPh₂CH₂Ph), –17.6 (triphos), –143.5 (septet, $J = 712$, PF₆). ¹H NMR (CD₂Cl₂): δ 7.54–7.49 (m, 6H, Ph), 7.31–7.24 (m, 10H, Ph), 7.07 (t, $J = 7.5$, 13H, Ph), 6.95 (br, 14H, Ph), 6.64 (d, $J = 8.5$, 2H, Ph), 3.99 (d, $J = 3.5$, 2H, CH₂), 2.62 (6H, CH₂), 1.67 (d, $J = 3.5$, 3H, CH₃). ¹³C{¹H} NMR (CD₂Cl₂): δ 134.5 (m, Ph), 134.0 (d, $J = 14$, Ph), 133.5 (d, $J = 7$, Ph), 132.2 (q, $J = 6$, Ph), 131.9 (br, Ph), 131.0 (d, $J = 2$, Ph), 130.3 (Ph), 130.2 (d, $J = 4$, Ph), 129.2 (m, Ph), 129.1 (Ph), 128.5 (d, $J = 2$, Ph), 127.3 (d, $J = 2$, Ph), 39.1 (m, CH₃), 37.9 (m, CH₂–P), 37.2 (br, MeC), 35.9 (m, CH₂–triphos).

[Cu(triphos)(PPh₂CH₂Cl)][PF₆] (17). A slurry of [Cu(triphos)(NCMe)][PF₆] (**2**; 155 mg, 0.178 mmol) in 1 mL of THF was treated with a solution of PPh₂CH₂Cl (50 mg, 0.21 mmol) in 2 mL of THF resulting in a clear, homogeneous solution, which was stirred for 1 h, then pumped down under vacuum. The residue was washed with petroleum ether (2 × 10 mL) to remove the excess phosphine and redissolved in 3 mL of CH₂Cl₂. The solution was then passed through Celite and recrystallized by layering the filtrate with petroleum ether at –30 °C yielding a white solid (187 mg, 0.175 mmol, 99%). Crystals suitable for X-ray diffraction were obtained by dissolving the sample in warm ethanol and allowing it to slowly cool at –30 °C.

Anal. Calcd. for C₅₄H₅₁ClCuF₆P₅: C, 60.74; H, 4.81. Found: C, 60.92; H, 4.40. HRMS m/z calcd for C₅₄H₅₁P₄ClCu (M⁺): 921.1926. Found: 921.1923. ³¹P{¹H} NMR (CD₂Cl₂): δ 11.6 (Ph₂PCH₂Cl), –16.7 (triphos), –143.5 (septet, $J = 711$, PF₆). ¹H NMR (CD₂Cl₂): δ 7.60–7.56 (m, 6H, Ph), 7.37–7.33 (m, 4H, Ph), 7.29 (t, $J = 7.5$, 6H, Ph), 7.05 (t, $J = 7$, 12H, Ph), 6.96 (br, 12H, Ph), 4.46 (2H, Ph₂PCH₂Cl), 2.64 (6H, CH₂–triphos), 1.68 (3H, CH₃). ¹³C{¹H} NMR (CD₂Cl₂): δ 134.2 (m, Ph), 133.4 (d, $J = 13$, Ph), 132.2 (dd, $J = 5$, 10, Ph), 131.6 (d, $J = 1$, Ph), 130.6–130.4 (m, Ph), 130.4 (Ph), 129.5 (d, $J = 9$, Ph), 129.2 (dd, $J = 3$, 6, Ph), 40.6 (m, Ph₂PCH₂Cl), 39.1 (q, $J = 11$, CH₃), 37.2 (m, CH₃C), 36.0 (m, CH₂–triphos).

[Cu(XantPhos)(PPh₂Ph)][PF₆] (18). A slurry of [Cu(XantPhos)(NCMe)][PF₆] (**3**; 200 mg, 0.24 mmol) in 2 mL of THF was treated with a solution of PPh₂Ph (45 mg, 0.24 mmol) in 2 mL of THF. The resulting clear solution was stirred for 1 h and then pumped down under vacuum. The residue was washed with petroleum ether (2 × 10 mL) and then recrystallized from methylene chloride layered with petroleum ether at –30 °C affording a white solid (220 mg, 0.226 mmol, 93%). ³¹P and ¹H NMR spectra at room temperature were very broad, consistent with a dynamic process; on cooling to –70 °C, the peaks remained broad, and more of them appeared.

Anal. Calcd. for C₅₁H₄₃CuF₆OP₄: C, 62.93; H, 4.45. Found: C, 62.99; H, 4.44. HRMS m/z calcd for C₅₁H₄₃CuOP₃ (M⁺): 827.1823. Found: 827.1816. ³¹P{¹H} NMR (CD₂Cl₂): δ –9.4 (broad with a significant shoulder), –28.2 (broad), –143.5 (septet, $J = 711$, PF₆). ¹H NMR (CD₂Cl₂): δ 7.71 (d, $J = 7$), 7.41 (broad), 7.24 (v. broad triplet with broad shoulder, $J = 8$), 6.68 (broad), 5.94 (v. broad d, $J = 327$, PH), 1.95, 1.72 (broad). The broadness of these peaks precluded meaningful integration.

[Cu(XantPhos)(PPh₂CH₂Ph)][PF₆] (19). A solution of [Cu(XantPhos)(NCMe)][PF₆] (**3**; 50 mg, 0.060 mmol) in 1 mL of CH₂Cl₂ was treated with PPh₂CH₂Ph (**4**; 17 mg, 0.060 mmol) in 1 mL of CH₂Cl₂ and stirred for 1 h. The reaction mixture was pumped down under vacuum. The residue was washed with petroleum ether (2 × 10 mL), redissolved in 3 mL of methylene chloride and passed through Celite. The transparent CH₂Cl₂ solution was then layered with petroleum ether and cooled to –30 °C resulting in the precipitation of a white crystalline solid (56 mg, 0.053 mmol, 88%). X-ray quality crystals were obtained by slow diffusion of petroleum vapors into a methylene chloride solution at –30 °C.

Anal. Calcd. for C₅₈H₄₉CuF₆OP₄: C, 65.51; H, 4.64. Found: C, 64.97; H, 4.51. HRMS m/z calcd for C₅₈H₄₉CuOP₃ (M⁺): 917.2292. Found: 917.2322. ³¹P{¹H} NMR (CD₂Cl₂): δ –0.6 (t, $J = 98$, PPh₂CH₂Ph), –12.2 (d, $J = 98$, XantPhos), –143.6 (septet, $J = 711$, PF₆). ¹H NMR (CD₂Cl₂): δ 7.76 (dd, $J = 1.5$, 7.5, 2H, Ph), 7.38 (t, $J = 7.5$, 4H, Ph), 7.33 (m, 2H, Ph), 7.26 (t, $J = 7.5$, 2H, Ph), 7.17 (t, $J = 7.5$, Ph), 7.14–7.12 (m, Ph), 7.10–7.06 (m, 17H total for 7.17–7.06, Ph), 6.97–6.96 (m, 4H, Ph), 6.94–6.90 (m, 8H, Ph), 6.71–6.69 (m, 2H, Ph), 3.47 (d, $J = 7.5$, 2H, Ph), 1.75 (Me, 6H). ¹³C{¹H} NMR (CD₂Cl₂): δ 154.2 (t, $J = 6$, Ph), 135.0 (Ph), 133.5 (t, $J = 2$, Ph), 133.1 (t, $J = 8$, Ph), 132.3 (d, $J = 4$, Ph), 132.2 (Ph), 130.9 (Ph), 129.6–129.2 (overlapping peaks, Ph), 129.2 (Ph), 129.1 (d, $J = 6$, Ph), 128.9 (Ph), 127.6 (d, $J = 3$, Ph), 125.6 (m, Ph), 118.5 (t, $J = 16$, Ph), 36.0 (CMe₂), 33.0 (d, $J = 16$, CH₂), 29.0 (CMe₂).

[Cu(dtbp)(PPh₂Ph)(OTf)] (20a). A solution of Cu(dtbp)(OTf) (**6**; 200 mg, 0.40 mmol) in 2 mL of CH₂Cl₂ was treated with a solution of PPh₂Ph (74 mg, 0.40 mmol) in 2 mL of CH₂Cl₂. The yellow-orange homogeneous solution was stirred for 1 h, then pumped down under vacuum. The resulting residue was washed with petroleum ether (2 × 10 mL). The crude product was recrystallized from methylene chloride layered with petroleum ether at –30 °C, giving a yellow solid (252 mg, 0.365 mmol, 92%).

Anal. Calcd. for C₃₃H₃₅CuF₃N₂O₃PS: C, 57.34; H, 5.10; N, 4.05. Found: C, 56.94; H, 5.00; N, 3.99. HRMS m/z calcd for C₃₂H₃₅N₂PCu (M⁺): 541.1834. Found: 541.1833. ³¹P{¹H} NMR (CD₂Cl₂): δ –24.9. ¹H NMR (CD₂Cl₂): δ 8.65 (d, $J = 8.5$,

2H, dtbp), 8.12 (d, $J = 8.5$, 2H, dtbp), 8.10 (2H, dtbp), 7.53–7.50 (br m, 2H, P-Ph), 7.42–7.36 (br m, 8H, P-Ph), 6.40 (d, $J = 341$, 1H, PH), 1.60 (18H, *t*-Bu). $^{13}\text{C}\{^1\text{H}\}$ NMR (CD_2Cl_2): δ 170.3 (Ar), 143.0 (Ar), 140.0 (Ar), 133.7 (d, $J = 12.5$, Ar), 131.5 (Ar), 129.7 (d, $J = 10$, Ar), 128.0 (Ar), 126.7 (Ar), 123.2 (Ar), 38.5 ($\text{C}(\text{CH}_3)_3$), 30.6 ($\text{C}(\text{CH}_3)_3$). $^{19}\text{F}\{^1\text{H}\}$ NMR (CD_2Cl_2): δ -79.2.

[Cu(dtbp)(PPh₂)(Cl)] (20b). A solution of Cu(dtbp)(Cl) (5; 100 mg, 0.26 mmol) in 2 mL of CH_2Cl_2 was treated with a solution of PPh₂ (48 mg, 0.26 mmol) in 1 mL of CH_2Cl_2 . The reaction mixture remained orange and was stirred for 1 h. The solution was pumped down under vacuum, washed with petroleum ether (2 × 10 mL), and recrystallized from CH_2Cl_2 layered with petroleum ether at -30 °C to afford an orange solid (94 mg, 0.16 mmol, 62%).

$^{31}\text{P}\{^1\text{H}\}$ NMR (CDCl_3): δ -33.2. ^1H NMR (CDCl_3): δ 8.30 (d, $J = 8.5$, 2H, dtbp), 7.94 (d, $J = 8$, 2H, dtbp), 7.80 (2H, dtbp), 7.56 (m, 4H, Ph), 7.34 (m, 2H, Ph), 7.25 (m, 4H, Ph), 5.85 (d, $J_{\text{PH}} = 313$, 1H, PH), 1.83 (18H, *t*-Bu).

Stoichiometric Deprotonation/Alkylation of [Cu(triphos)-(PPh₂)]PF₆ (12): PhCH₂Br. An NMR tube was charged with a solution of [Cu(triphos)(PPh₂)]PF₆ (12; 50 mg, 0.049 mmol) in 1 mL of CD_2Cl_2 . Neat PhCH₂Br (6 μL , 0.05 mmol) was added via syringe, followed by a solution of NaOSiMe₃ (6 mg, 0.05 mmol), and the reaction was monitored by ^1H and ^{31}P NMR spectroscopy. After 15 min, complete conversion to [Cu(triphos)(PPh₂CH₂Ph)]PF₆ (16) was observed.

Stoichiometric Deprotonation/Alkylation of [Cu(triphos)-(PPh₂)]PF₆ (12): CD₂Cl₂. A solution of [Cu(triphos)(PPh₂)]PF₆ (12; 50 mg, 0.049 mmol) in less than 1 mL of CD_2Cl_2 was placed in an NMR tube, which was capped with a rubber septum and sealed with Parafilm. The NMR tube was then cooled to -78 °C in a dry ice/acetone bath and injected via syringe with a solution of NaOSiMe₃ (55 mg, 0.49 mmol) in less than 1 mL of CD_2Cl_2 . The reaction mixture was kept at -78 °C and analyzed by low temperature NMR spectroscopy at 10 °C intervals beginning at -70 °C. Formation of [Cu(triphos)(PPh₂CD₂Cl)]PF₆ (17-D₂) was first observed starting at -40 °C. On warming to room temperature, this complex was formed as the major product and identified by comparison of its ^{31}P and ^1H NMR spectra to independently prepared 17 (as expected, for 17-D₂, the CH₂ ^1H NMR signal was not observed). Some decomposition products were also observed by ^{31}P NMR (δ -8.8, -19.8, -21.3).

Ion-Exchange; Preparation of 12-B(Ar_F)₄. A solution of [Cu(triphos)(PPh₂)]PF₆ (12; 100 mg, 0.098 mmol) in CH_2Cl_2 was treated with a slurry of K[B(Ar_F)₄] (89 mg, 0.098 mmol) in approximately 25 mL of water. The mixture was transferred to a separatory funnel and vigorously shaken. The layers were distinct, but the interface was very cloudy even after long periods of equilibration. The organic layer was separated, washed (3 × 25 mL) with water, and dried over MgSO₄. The solution was passed over a frit, and the filtrate was pumped down yielding an oily solid (22 mg, 0.012 mmol, 13%). The low yield appeared to arise from poor separation of 12-B(Ar_F)₄ from the aqueous layer. The $^{31}\text{P}\{^1\text{H}\}$ NMR (CDCl_3) spectrum (δ -16.5) confirmed that no PF₆⁻ was present.

^1H NMR (CDCl_3): δ 7.73 (br, 8H, BAr_F), 7.64–7.60 (overlapping doublets, $J = 11$, 4H, Ar), 7.52 (br, 4H, BAr_F), 7.49 (overlapping triplet, $J = 7$, 2H, Ar), 7.34 (m, 4H, Ar), 7.19 (t, $J = 7$, 6H, Ar), 6.98–6.92 (br m, 24H, Ar), 6.52 (dq, $J = 7$, 316, 1H, PH), 2.52 (br, 6H, CH₂), 1.26 (3H, CH₃).

Deprotonation of 12-B(Ar_F)₄; Generation of Cu(triphos)-(PPh₂) (22). A solution of [Cu(triphos)(PPh₂)]B(Ar_F)₄ (12-B(Ar_F)₄; 21 mg, 0.12 mmol) in less than 1 mL of *d*₈-THF was placed in an NMR tube, which was capped with a rubber septum, and sealed with Parafilm. The NMR tube was cooled to -78 °C in a dry ice/acetone bath and injected via syringe with a solution of NaOSiMe₃ (14 mg, 0.12 mmol) in 1 mL of *d*₈-THF. The reaction mixture was kept at -78 °C and analyzed by low temperature NMR spectroscopy. Complex 22 was observed at -70 and -50 °C by ^{31}P NMR spectroscopy. Warming to -40 °C

led to some decomposition, with widespread decomposition occurring at -30 °C. Some of the decomposition products identified by ^{31}P NMR spectroscopy at -30 °C were triphos (δ -26.1) and PPh₂ (δ -40.3), along with several other unidentified peaks at δ -15.8, -18.6, -20.6, and -34.4. At room temperature, the ^{31}P NMR spectrum showed no signals corresponding to 22; however, triphos (δ -25.0) and PPh₂ (δ -39.9) were observed along with several unidentified peaks at -20.9, -23.9, -26.8, and -34.0 ppm.

NMR data for Cu(triphos)(PPh₂) (22): $^{31}\text{P}\{^1\text{H}\}$ NMR (*d*₈-THF, -50 °C): δ -23.4 (d, $J = 27$, triphos), -30.3 (q, $J = 27$, PPh₂). ^1H NMR (*d*₈-THF, -50 °C): δ 7.86 (br, 4H, BAr_F), 7.69 (br, 8H, BAr_F), 7.30 (br, 12H, Ph), 7.07 (t, $J = 7$, 8H, Ph), 6.91 (t, $J = 7$, 12H, Ph), 6.81 (br, 8H, Ph), 2.43 (br, 6H, CH₂), 1.53 (br, 3H, CH₃).

Ligand Substitution: Equilibrium Between [Cu(triphos)-(PPh₂CH₂Ph)]PF₆ (16), PPh₂, [Cu(triphos)(PPh₂)]PF₆ (12) and PPh₂CH₂Ph (4). A solution of [Cu(triphos)(PPh₂)]PF₆ (12; 50 mg, 0.049 mmol) in less than 1 mL of CD_2Cl_2 was treated with a solution of PPh₂CH₂Ph (4; 14 mg, 0.049 mmol) in 1 mL of CD_2Cl_2 and transferred to an NMR tube. The ^{31}P NMR spectrum was monitored over the course of several hours, but did not change from the initial spectrum taken less than 15 min after the addition of PPh₂CH₂Ph. An identical spectrum resulted from treatment of [Cu(triphos)(PPh₂CH₂Ph)]PF₆ (16; 50 mg, 0.045 mmol) with 1 equiv of PPh₂ in CD_2Cl_2 . From integration of the broad ^{31}P NMR signals observed in both experiments, $K_{\text{eq}} = 8(2)$, favoring coordination of PPh₂.

Ligand Substitution: Equilibrium Between [Cu(triphos)-(PPh₂CH₂Cl)]PF₆ (17), PPh₂, [Cu(triphos)(PPh₂)]PF₆ (12) and PPh₂CH₂Cl (7). A solution of [Cu(triphos)(PPh₂)]PF₆ (12; 52 mg, 0.051 mmol) in less than 1 mL of CD_2Cl_2 was treated with a solution of PPh₂CH₂Cl (7; 12 mg, 0.051 mol) in 1 mL of CD_2Cl_2 . The resulting homogeneous solution was transferred to an NMR tube, then analyzed by ^{31}P NMR spectroscopy after 30 min. An identical spectrum resulted when the mixture was generated by treatment of [Cu(triphos)(PPh₂CH₂Cl)]PF₆ (17; 57 mg, 0.054 mmol) with PPh₂ (10 mg, 0.054 mmol) in CD_2Cl_2 . From integration of the broad ^{31}P NMR signals observed in both experiments, $K_{\text{eq}} = 7(2)$, favoring coordination of PPh₂.

DFT Computations. Gas phase structures were optimized using the hybrid B3LYP functional⁴¹ and the triple- ζ LACV3P**++ basis set,⁴² which uses extended core potentials on heavy atoms and a 6-311G**++ basis for other atoms, as implemented in the Jaguar suite of programs (Jaguar, versions 7.0–7.5, Schrödinger, LLC, New York, NY: 2007–2009). All computed structures were confirmed as energy minima by calculating the vibrational frequencies by second derivative analytic methods, and confirming the absence of imaginary frequencies. Thermodynamic quantities were calculated assuming an ideal gas, and are zero point energy corrected.

Acknowledgment. D.S.G. thanks the National Science Foundation for support. R.P.H. also thanks the National Science Foundation.

Supporting Information Available: Additional experimental details, details of the X-ray crystallographic studies, including crystallographic information files (CIF), additional NMR spectra, and details of the DFT calculations. This material is available free of charge via the Internet at <http://pubs.acs.org>.

(41) (a) Lee, C.; Yang, W.; Parr, R. G. *Phys. Rev. B* **1988**, *37*, 785–789. (b) Stephens, P. J.; Devlin, F. J.; Chabalowski, C. F.; Frisch, M. J. *J. Phys. Chem.* **1994**, *98*, 11623–11627. (c) Becke, A. D. *J. Chem. Phys.* **1993**, *98*, 5648–5652. (d) Becke, A. D. *J. Chem. Phys.* **1993**, *98*, 1372–1377.

(42) (a) Dunning, T. H.; Hay, P. J. In *Modern Theoretical Chemistry, Vol. 4: Applications of Electronic Structure Theory*; Schaefer, H. F., III, Ed.; Plenum: New York, 1977. (b) Hay, P. J.; Wadt, W. R. *J. Chem. Phys.* **1985**, *82*, 270–283. (c) Hay, P. J.; Wadt, W. R. *J. Chem. Phys.* **1985**, *82*, 299–310. (d) Wadt, W. R.; Hay, P. J. *J. Chem. Phys.* **1985**, *82*, 284–298.